PHOTOCATALYTIC DEGRADATION OF SUNSET YELLOW DYE OVER ZINC OXIDE NANOPARTICLES UNDER FLUORESCENT LIGHT IRRADIATION

LAM LEK SIONG

UNIVERSITY TUNKU ABDUL RAHMAN

PHOTOCATALYTIC DEGRADATION OF SUNSET YELLOW DYE OVER ZINC OXIDE NANOPARTICLES UNDER FLUORESCENT LIGHT IRRADIATION

Lam Lek Siong

A project report submitted in partial fulfilment of the requirements for the award of Bachelor of Engineering (Hons) Petrochemical Engineering

Faculty of Engineering and Green Technology
University Tunku Abdul Rahman

May 2016

DECLARATION

I here declare that this project report is based on my original work except for citations and quotations which have been duly acknowledged. I also declare that it has not been previously and concurrently submitted for any other degree or award at UTAR or other institutions.

Signature :_____

Name :_____

ID No. :_____

Date :_____

APPROVAL FOR SUBMISSION

I certify that this project report entitled **''PHOTOCATALYTIC DEGRADATION OF SUNSET YELLOW DYE OVER ZINC OXIDE NANOPARTICLES UNDER FLUORESCENT LIGHT IRRADIATION''** was prepared by **LAM LEK SIONG** has met the required standard for submission in partial fulfilment of the requirements for the award of Bachelor of Engineering (Hons) Petrochemical Engineering at University Tunku Abdul Rahman.

Approved by,

Signature :_____

Supervisor :_____

Date :_____

ACKNOWLEDGEMENTS

I would like to thank everyone who had contributed to the successful completion of this project. I would like to express my humblest gratitude to my research supervisor, Dr. Sin Jin Chung for his invaluable advises guidance and his enormous patience throughout the development of the research.

In addition, I would like to express my gratitude to my loving parents and friends who helped and given me encouragement throughout the project.

PHOTOCATALYTIC DEGRADATION OF SUNSET YELLOW DYE OVER ZINC OXIDE NANOPARTICLES UNDER FLUORESCENT LIGHT IRRADIATION

ABSTRACT

Water pollution is a concerning issue faced by the world. Among the pollutants, dyes have become the focus of the environmental issue. Dyes have high durability due to their complex molecular structure and can give toxic effects to human and animal even at low concentration. Heterogeneous photocatalysis using zinc oxide (ZnO) semiconductor has recently been emerged as an effective way to degrade the organic pollutants including dyes. In this study, commercial ZnO nanoparticles have been used for the photocatalytic degradation of sunset yellow (SSY) dye under fluorescent light irradiation. The ZnO nanoparticles were characterized by using X-ray diffraction (XRD), fourier transform infrared spectroscopy (FTIR) and transmission electron microscopy (TEM). The XRD pattern revealed the typical hexagonal wurzite structure of ZnO particles. The FTIR spectrum has identify that the photocatalysts were indeed ZnO. The TEM image showed that the ZnO nanoparticles were irregularly shaped the particles size range was determined to be from 153nm to 283 nm. Effects of operating parameters such as initial SSY concentration, ZnO catalyst loading and solution pH were also studied. Degradation efficiency of SSY decreases as the initial SSY concentration increased. The optimal ZnO catalyst loading was found to be 7 g/L. The unadjusted solution pH of SSY which was 5.8 was favourable for photocatalytic degradation and was the optimum solution pH. Finally, the effect of various scavengers was also investigated to determine the role

of the active species in the reaction mechanism. Super oxide anion radicals ($O_2^{\bullet -}$) was observed to be the main reactive species in this study.

TABLE OF CONTENTS

CHAPTER

LIST OF TABLES

LIST OF FIGURES

LIST OF SYMBOLS/ABBREVIATION

AOP	Advanced Oxidation Process
CO_2	Carbon Dioxide
C_o	Concentration of dye after 30 min of dark run
C.I	Colour Index
C_t	Concentration of dye at reaction time, *t*
CdS	Cadmium Sulfide
CdSe	Cadmium selenide
e_{cb}^-	Excited electron
eV	Electron volt
Fe_2O_3	Iron (III) oxide
FTIR	Fourier transform infrared spectroscopy
$O_2•^-$	Superoxide anion radical
•OH	Hydroxyl radical
OH^-	Hydroxyl ions
GaAs	Gallium arsenide

h_{vb}^{+}	Positive hole
H_2O	Water
H_2O_2	Hydrogen Peroxide
H_2SO_4	Sulfuric Acid
NaOH	Sodium Hydroxide
pH_{zpc}	pH of zero point charge
pK_a	Acid dissociation constant
R	Pollutant
SnO_2	Tin Oxide
SO_4^{2-}	Sulphate anions
$SO_4^{\bullet -}$	Sulphate radicals
SSY	Sunset yellow
TEM	Transmission electron microscopy
TiO_2	Titanium Oxide
UV	Ultra violet
WO_3	Tungsten Oxide
XRD	X-ray diffraction
ZnO	Zinc Oxide
ZnS	Zinc sulfide
ZrO_2	Zirconium Dioxide

LIST OF APPENDICES

CHAPTER 1

INTRODUCTION

1.1 Background of Study

In the present, the population and industrial developments in all over the world are growing rapidly. This phenomenon leads to major global problems which are the environment pollutions and water pollution is one of them. Water is one of the most abundant resources on earth. In fact, approximately 70 % of the earth's surface is covered by water and water also existed in the air and even in living organisms. Water is essential for all the living organisms as they are impossible to survive without water. Thus, the quality and quantity of the water are a major concern. According to World Wildlife Fund, water pollution can be defined as the degradation of water quality due to toxic substances entering and remaining in the water bodies like oceans, rivers and lakes (World Wildlife Fund, 2015). Since living organism is highly dependent on water, the change in water quality can certainly affect the ecosystems and our daily lives.

In 2008, the Department of Environmental has identified 17,633 water pollution point sources in Malaysia (Alfroz et al, 2014). The sewage treatment plants made up of the most point sources which were 54.1 % and manufacturing industries' was 38.7 %. The rest of the point sources were animal farms (4.48 %) and agro-based industries (2.78 %). From the statistics, the wastewater from sewage and industrial effluent were considered as the major contributors to water pollution. In addition, non-point sources were also contributed in the pollution of water. Non-point sources can be defined as diffused sources like surface runoffs and agricultural activities (Department of Environment, 2015). The act that was enforced to protect the environment was Environmental Quality Act 1974 which was Act 127 of the

Laws of Malaysia. This act is defined as an act relating to the prevention, abatement, control of pollution and enhancement of the environment, and for purposes connected therewith (The Commissioner of Law Revision, Malaysia, 2006). Even with the enforcement of this act, the pollution issue is still occurring.

According to Lenntech (2015), the water pollutants can be classified as organic pollutants, inorganic pollutants, metals, and radioactive isotopes. Examples of organic pollutants are oils, dyes and detergents. Fertilizers like nitrates and phosphates can be considered as inorganic pollutants. On the other hand, metals such as lead, calcium, potassium, and manganese are also grouped into pollutants. As for radioactive isotopes, four types of particles are produced when the isotopes decays which are alpha, beta, gamma, and neutrons. These particles have varied penetration power and can cause damage to living tissues based on the types. The pollutants have different ways to affect living organisms depending on the pollutants' properties. Some pollutants can poison the organisms via entering the organisms' body and the effect can range from causing sickness to fatal. Apart from that, pollutants that are hard to be bio-degraded can increase the biochemical oxygen demand of the water and thus, decreasing the available oxygen in the water and consequently lead to the lack of oxygen for the aquatic lives (Lenntech, 2015).

Among the pollutants, the dyestuffs and colorants have become the focus of the environmental issue (Sakthivel et al, 2002). Dyes are usually hard to be decomposed in water due to their composite molecular structures that make them stable against light and resist biodegradation (Jo & Tayade, 2014). Main source of dyes came from industrial processes such as textile, leather, cosmetic, paper, food processing, distillation, fabric, plastic, ink, electroplating, agriculture research and pharmaceuticals that involved the use of dyes (Lam et al, 2012; Jo & Tayade, 2014; Suresh, Vijaya & Kennedy, 2014; Zangeneh et al, 2014). The global production of dyes was 7×10^5 tonnes per year and around 15 % was lost during the dying process and was released in the effluent (Lam et al, 2012; Jo & Tayade, 2014; Zangeneh et al, 2014). The contamination of coloured wastewater even at low concentrations can give toxic effects to human and animals as well as reducing the light penetration in contaminated water (Jo & Tayade, 2014; Zangeneh et al, 2014). Therefore, there exist needs for developing treatment techniques that can lead to the complete destruction of the dye molecules from waste stream.

In recent years, an emerging advanced oxidation process known as photocatalysis has attracted considerable attention as an alternative method to deal with the dye pollutants. The advanced oxidation process is based on the generation of active oxidizing species like the hydroxyl radicals (•OH), superoxide anion radicals ($O_2•^-$) and hydrogen peroxide (H_2O_2) to attack the organic dyes pollutants (Ribeiro et al, 2015). The photocatalysis method consisted of three main components: light, catalyst, and oxygen. Semiconductors like ZnO, TiO_2, CdS and ZnS are used as the catalysts which can be activated by irradiation of ultraviolet light and/ or sun light to generate powerful oxidizing agents with the help of oxygen (Chong et al, 2010; Ribeiro et al, 2015). Photocatalysis came with the advantages of having low operating cost, worked under ambient pressure and temperature, and possibility to achieve complete mineralization (Chong et al, 2010). In addition, no secondary pollution occurred when the dyes are completely mineralized and no post treatment or disposal is needed. The end products of the photocatalytic degradation are usually harmless and eco-friendly (Sakthivel et al, 2002). Apart from that, the semiconductor itself is an economic material. Thus, the photocatalysis method is getting popular as an effective means to treat the dye wastewater.

1.2 Problem Statement

With all the problems given rise by the water pollution through dye wastewater, major concerns were put into this issue. Thus, various water treatment technologies have been developed so as to deal with the issue. The three main types of methods for water treatment are biological, chemical and physical. Biological water treatments involved the use of microorganisms to biodegrade the pollutants in the water. Examples of such treatments are aerobic and anaerobic water treatments (Mittal, 2011). However, the efficiency of biological treatment is insufficient because of the non-biodegradability of dyes. Thus, the biodegradation will be time consuming and incomplete (Zangeneh et al, 2014). The chemical water treatments mainly involved the reactions between the selected chemicals and the pollutant and killing bacteria or viruses with chemicals. Examples of such treatments are chlorination and ozonation. However, the methods have disadvantages such as potentially hazardous chlorinated by products can be produced as well as ozone's toxicity and instability

(United States Environmental Protection Agency, 1999; Chong et al, 2010). Furthermore, chemical methods can be very expensive as amount of chemicals required is high and large amount of sludge can be produced (Zangeneh et al, 2014). As for physical water treatment methods, they involved trapping and separating the pollutant and water through physical means. Carbon adsorption, reverse osmosis and ultrafiltration are some of the examples for such methods. Even though the water is free of dye after the treatment processes, the pollutants still existed and are not eliminated due to the non-destructive nature of the processes. This will result in secondary pollution which is undesirable in the long run. In addition there are other limitations such as the high cost and the carbon adsorption required disposal of spent carbon (Zangeneh et al, 2014).

On the other hand, the photocatalytic degradation method can potentially mineralize the dye completely. Furthermore, it has lower requirements compared to the other processes as the photocatalysis can be activated under sunlight and no extreme conditions are required. With the limitations of the other methods, photocatalysis can be a good alternative way to eliminate the dye pollutants. Among the semiconductors, TiO_2 was considered as one of the most popular catalysts because of its high activity, good photo and chemical stability, non-toxic, biologically inert and water insolubility (Zangeneh et al, 2014). Even though the TiO_2 was widely used as the catalyst, the ZnO can substitute the TiO_2 due to its similar photodegratation mechanism and lower cost (Daneshwar, Salari & Khataee, 2004; Chakrabarti & Dutta, 2004). In addition, it has also been found that ZnO powder has better quantum efficiency compared to TiO_2 powder and led to higher photocatalytic activities (Chakrabarti & Dutta, 2004).

1.3 Objectives

The aim of this research is to observe the photocatalytic degradation of sunset yellow (SSY) dye under fluorescent light using ZnO photocatalyst. The objectives of this research include:

1. To characterize the ZnO photocatalyst.

2. To study the effects of the operating parameters such as catalyst loading, initial dye concentration and solution pH on the photocatalytic degradation of SSY using ZnO photocatalyst.
3. To study the effect of radical scavengers on the photocatalytic degradation of SSY over ZnO photocatalysts

1.4 Scope of Study

This study focused on the photocatalytic degradation of SSY using ZnO as the photocatalysts. The photocatalysts are characterized by X-ray diffraction (XRD), fourier transform infrared spectroscopy (FTIR) and transmission electron microscopy (TEM). In addition, key operating parameters such as catalyst loading (0.5 g/L – 9.0 g/L), solution pH (3.1-10.5), and initial dye concentration (8 mg/L – 32 mg/L) on the degradation of SSY will also be studied. Finally, the effects of ethanol, benzoquinone and sodium oxalate as radical scavengers are also studied on the photocatalytic degradation of SSY over ZnO.

CHAPTER 2

LITERATURE REVIEW

2.1 Dye Classification

There are a number of different classes of dyes based on their applications. Examples of the dyes classes are reactive dyes, direct dyes, disperse dyes, vat dyes anthraquinone dyes, sulfur dyes, cationic azo dyes, cationic methine dyes, acid dyes, solvent dyes, metal-complex dyes, naphthoquinone and benzoquinone dyes (Lam et al, 2012; Hunger, 2013). Among these dyes, the acid dyes class is considered as the largest in the colour index (Lam et al, 2012). The dying process of acid dye is carried out in acidic aqueous solution with a typical pH value of 2 to 6 and thus, the term 'acid dyes'. Acid dyes can be further classified into three groups depending on the affinity difference which is related to molecular size:

1) Leveling dyes are molecules with relatively small size which are able to form a salt-like bond with the protein fibre.
2) Milling dyes are molecules with a large volume, for which salt formation with the fibre is just the secondary role and the adsorption forces between the protein fibre and the hydrophobic regions of the dye molecule predominate.
3) The dyes with intermediate molecular size are able to form a salt-like bond with the wool fibre as well as bonding to the fibre by intermolecular forces. This group of dyes has the properties lying in an intermediate position between those of the leveling and the milling dyes.

The main applications of the acid dyes are the dyeing and printing of wool, silk, polyamide, and basic-modified acrylics as well as dying food, leather, paper and fur. Acid dyes can include many types of compunds such as azoic, anthraquinone, triphenylmethane, and nitro dyes. However, they have a common characteristic

which is their water-soluble and ionic substituents. Among the compounds, the anionic azo dye is the mostly used type of dye (Lam et al, 2012; Hunger, 2013). The azo group dyes mainly consisted of a naphthalene ring linked to a second benzene ring through an azo bond (N=N). These rings can contain one, two, or three sulfonic groups. The azo dyes are the most commonly used synthetic dyes by the food industry especially the sunset yellow (SSY) (Pandey, Singh & Iyengar 2007; Gomes et al. 2013). Approximately one-half of all dyes produced are made up of azo dyes. In addition to food industry, they are applied in the textile, printing, paper, leather and cosmetic industries. The electron withdrawing groups in the azo dyes generate electron deficiency in the dye molecule and thus, made the dyes resisted to degradation. A lot of azo dyes and their breakdown products are harmful to living organisms (Singh, Singh & Singh, 2015).

2.1.1 Sunset Yellow Dye (SSY)

The SSY is a synthetic sulfonated monoazo dye (Ghoneim, El-Desoky & Zidan, 2011). The chemical structure of the SSY is shown in Figure 2.1.

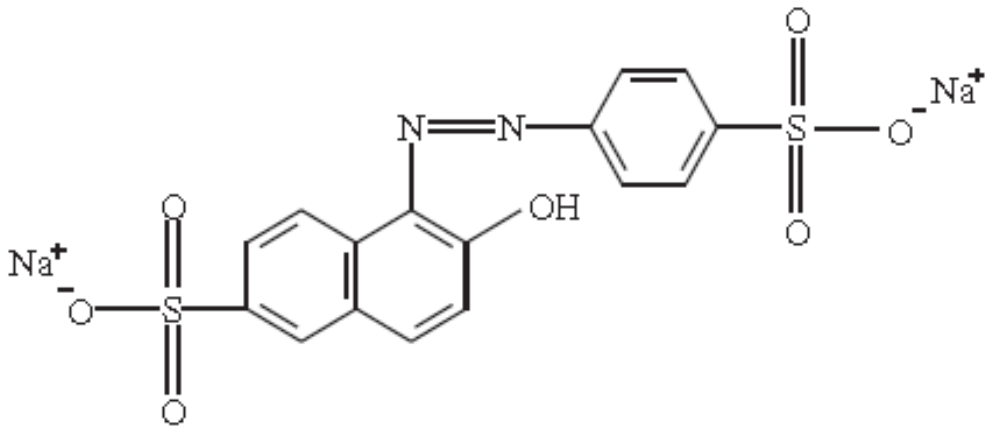

Figure 2.1: Chemcial Structure of SSY Azo Dye Molecule (Ghoneim, El-Desoky & Zidan, 2011)

The SSY food dye is synthesized from coal tar and azoic paints (Gomes et al. 2013). The information on the dye is tabulated in Table 2.1.

Table 2.1: Information on SSY Azo Dye (Sabnis, 2010)

CA Index Name	**2-Naphthalenesulfonic acid, 6-hydroxyl-5-[2-(4-sulfophenyl)diazenyl]-,sodium salt (1:2)**
Alternative Names	Sunset Yellow FCF, C.I. Food Yellow 3, Orange Yellow 85, Sun Yellow, Orient Yellow 2, Water Yellow 2, Yellow 6, Twilight Yellow and etc
Emperical Formula	$C_{16}H_{10}N_2Na_2O_7S_2$
Molecular Weight	452.37
Physical Form	Orange-red crystals
Solubility	Soluble in water and ethanol
Melting Point	390 ˚C (decompose)
Examples of Colouring Applications	Animal feed, bread, cereal, candies, beverages, bakery products, dietary supplement, soft drinks, soup, frozen food product, sweeteners, tattoos, skin, lips, tooth, hairs.
Examples of Biological Applications	Medical devices, treating dermatological disorders, mitochondrial diseases, bone metabolic diseases, and respiratory illness
Examples of Industrial Applications	Thermoplastics, inks, paints, cleansing products, batteries, textiles, coloured bubbles, toys.

The SSY can lead to allergic reactions in individuals that have sensibility to the SSY's components or have aspirin intolerance. The symptoms caused are gastric upset, diarrhea, vomiting, anaphylactic shock, vasculitis, nettle rash (urticaria) and swelling of the skin (angioedema). Furthermore, it can intensify the aggressive behaviour in children as well as triggering serious allergic reactions in people that are sensitive to paracetamol, acetylsalicylic acid, and sodium benzoate (Ghoneim, El-Desoky & Zidan, 2011; Gomes et al. 2013)

2.2 Methods of Dye Removal

Typically, there is only 0.6 to 0.8 g L^{-1} of dye in the effluent. However, it is very durable and is sufficient to cause pollution (Saratale et al, 2011). Thus, it is important to develop effective dye effluent treatment methods. There are already a lot of feasibility studies regarding the methods. A number of conventional biological, chemical, and physical methods are currently available to be used to treat the dye effluents (Golob, Vinder & Simonic, 2005).

2.2.1 Biological Methods

The biological treatment technique is regarded as one of the most common and widespread methods used in dye effluent treatment. It has been used for more than 150 years (Hunger, 2003). In this method, the selected microorganisms adapt themselves to the pollutant and eventually develop new resistant strains. The strains are able to let the microorganisms to transform the toxic wastes into less harmful forms. Microorganisms such as bacteria, fungi, algae, actinomycetes, yeasts and plant are able to decolourise the dye effluent (Saratale et al, 2011). The treatment can be further classified into two types which are aerobic and anaerobic. The aerobic treatments need oxygen so as to let the microbes to perform the biodegradation while the anaerobic do not need oxygen (Hunger, 2003).

The main flaw with the biological treatment is that the azo compound is xenobiotic so resistance against biodegradation is anticipated. It has already been reported that dyes resisted to biodegradation in conventional activated sludge treatment units (Pandey, Singh & Iyengar 2007; Saratale et al, 2011). Furthermore, the process took a long time and the operating temperature range was narrow (Verma, Dash & Bhunia, 2012). The isolation and preservation of new strains as well as the existing ones that can decompose dyes may probably increase the efficiency of bioremediation of dyes in the future (Forgacs, Cserháti & Oros, 2004).

2.2.2 Chemical Methods

Chemical methods such as the coagulation and flocculation have been conventionally used in wastewater treatment. In fact, the method is one of the most widely applied

techniques in textile wastewater treatment plants in many countries. The technique is able to be used either as a pre-treatment, post-treatment, or even as a main treatment process (Santos, Cervantes & Lier, 2007). Salts of aluminium and iron are the most widely used coagulants (Riera-Torres, Gutiérrez-Bouzán & Crespi, 2010; Khouni et al, 2011).This technique involved the use of chemical to modify the physical state of dissolved and suspended solids so as to remove it easily by processes such as sedimentation, flotation and filtration (Golob, Vinder & Simonic, 2005; Verma, Dash & Bhunia, 2012).

This treatment is usually used to remove organic substances and is effective in removing insoluble dyes. However, this method has flaws such as the low efficiency with respect to soluble dyes as well as the generation of large amount of sludge due to the flocculation of reagents and dye molecules (Allègre et al, 2006; Gao et al, 2007; Riera-Torres, Gutiérrez-Bouzán & Crespi, 2010; Verma, Dash & Bhunia, 2012). It has been reported that the coagulation/flocculation method were applied for colour removal of sulphur and disperse dyes successfully. On the other hand, organic dyes such as acid, direct, reactive and vat dyes have shown very low coagulation/flocculation capacity (Santos, Cervantes & Lier, 2007). The cost for the sludge treatment and disposal are high and the restrictions on their disposal have been increasing (Allègre et al, 2006). Additionally, the process usually required large inputs of chemicals which increased the operational cost even more (Santos, Cervantes & Lier, 2007). The rapid development of dye synthesis technology also continued to introduce a large number of new dyes with complex structures which made the selection of proper coagulant agents even more difficult (Verma, Dash & Bhunia, 2012).

Another chemical method is the chemical oxidation using ozone (O_3). This method usually involved the use of oxidizing agent which is ozone (O_3) to modify the chemical composition of dyes. The dyes can be degraded into less complex compound which is harmless compare to dyes (Santos, Cervantes & Lier, 2007; Verma, Dash & Bhunia, 2012; Ribeiro et al, 2015) However, the ozone has limited efficiency in decolourising non-soluble disperse and vat dyes with a low reaction rate (Santos, Cervantes & Lier, 2007; Verma, Dash & Bhunia, 2012). Another drawback is that the ozone is designed to attack the double bonds like the –N=N– bonds and the biodegradable compounds are not oxidized. Thus, the reduction of chemical

oxygen demand is low. Furthermore, the cost of the ozone as well as the installation of ozonation process are high (Allègre et al, 2006; Santos, Cervantes & Lier, 2007).

2.2.3 Physical Methods

There are many physical methods available for textile wastewater treatment. One of the classes of such methods is the membrane processes and they are being increasingly used in the dye removal process for the recovery of valuable compounds from the wastewater and the recycling of the water (Riera-Torres, Gutiérrez-Bouzán & Crespi, 2010). The membrane technology mainly revolved around the trapping or filtering the pollutant through physical means and thus, separating them with the effluent. The factors that determine the type and porosity of the filter are the specific temperature and chemical composition of the wastewaters (Verma, Dash & Bhunia, 2012). Reverse osmosis (RO), nanofiltration (NF), ultrafiltration (UF) and microfiltration (MF) are considered as membrane processes (Allegre et al, 2004; Allègre et al, 2006; Khouni et al, 2011).

However, the processes have flaws. One of the major problems is the decline of flux with time due to membrane fouling (Banerjee, DasGupta & De, 2007; Riera-Torres, Gutiérrez-Bouzán & Crespi, 2010; Khouni et al, 2011; Verma, Dash & Bhunia, 2012). In addition, membrane processes also required high cost and different pretreatments depending on the nature of the wastewater input. In physical treatment, the pollutants are merely transferred to another phase and are not destroyed which can result in secondary pollutions (Chong et al, 2010). The sludge will also need to be properly treated before being able to be disposed safely to the environment which led to more complicated operations and additional costs (Verma, Dash & Bhunia, 2012).

Another physical method is the adsorption technique. This method for dye treatment relied on the affinity of the dyes for adsorbents and thus, the adsorbents selection is important (Verma, Dash & Bhunia, 2012). There are also disadvantages of this technique that limited its use not only in dye effluent treatment but also in other water and wastewater treatments (Verma, Dash & Bhunia, 2012). The flaws of this technique are the disposal of spent adsorbents and high maintenance costs.

(Hunger, 2003; Allègre et al, 2006; Riera-Torres, Gutiérrez-Bouzán & Crespi, 2010; Verma, Dash & Bhunia, 2012).

2.3 Advanced Oxidation Process

With the drawbacks of the conventional treatment methods, an alternative technology has been proposed as substitution. This clean technology is known as advanced oxidation process (AOP). The basic principle of the process is the in situ generation of active oxidizing agents such as hydroxyl radicals (•OH), superoxide anion radicals ($O_2•^-$), hydroperoxyl radicals ($HO_2•$) and hydrogen peroxide (H_2O_2) to attack the organic pollutants (Azbar, Yonar & Kestioglu, 2004; Banerjee, DasGupta & De, 2007; Lam et al, 2012; Punzi et al, 2012; Ribeiro et al, 2015). These agents have excellent oxidizing power and can degrade organic pollutants to harmless compounds (Banerjee, DasGupta & De, 2007; Ribeiro et al, 2015). A common pathway for the degradation of organic compounds by the •OH radicals is shown in equations (2.1)-(2.4) (Azbar, Yonar & Kestioglu, 2004).

$$•OH + RH \rightarrow H_2O + R• \quad (2.1)$$

$$R• + H_2O_2 \rightarrow ROH + •OH \quad (2.2)$$

$$R• + O_2 \rightarrow ROO• \quad (2.3)$$

$$ROO \cdot + RH \rightarrow ROOH + R• \quad (2.4)$$

The production of the oxidizing species will be based on the type of AOPs being employed. Different processes have distinct fundamentals and one should choose an appropriate AOP depending on the specific characteristic of the target effluent. In general, the AOPs can be divided to homogeneous and heterogeneous processes, depending on whether the process is carried out in a single phase or the usage of a heterogeneous catalyst like metal supported catalysts, carbon materials or semiconductors such as ZnO, TiO_2, and WO_3 (Ribeiro et al, 2015). Most of the AOP are effective in treating dye effluent (Verma, Dash & Bhunia, 2012). It is possible to have near complete mineralization of the dyes as well as the intermediates with appropriate process selection. Thus, the post treatments are not needed and secondary pollutants are not produced. Therefore, it gave an edge over the conventional treating processes in which large amount of chemical or biological sludge are generated (Azbar, Yonar & Kestioglu, 2004).

2.4 Basic Principle of Photocatalysis

Among the AOPs, the heterogeneous photocatalysis is popular as an alternative method to treat the dye effluent. In 1972, Fujishima and Honda had described the photoelectrochemical decomposition of water under the irradiation of light and without applying any electricity using TiO_2 for the first time. Ever since the successful implementation of TiO_2 in the oxidation of cyanide ion in aqueous solution, the interest and attention on the photocatalytic processes' environmental applications have been increasing dramatically (Ribeiro et al, 2015). This process is considered as an AOP and involved the generation of active radicals in situ under ambient conditions via photocatalyst. The radicals can degrade the toxic compounds including dyes into harmless products such as CO_2 and H_2O (Ahmed et al, 2010). Basically, the process consisted of three main components: light, catalyst and oxygen. The typical photocatalysts are semiconductors like TiO_2, ZnO, GaP, Fe_2O_3, CdS and ZnS (Chong et al, 2010; Ribeiro et al, 2015).

The technique is effective because it is able to achieve near complete mineralization of various organic compounds (Rauf & Ashraf, 2009; Chong et al, 2010). Apart from that, the low cost of semiconductors made this process even more feasible (Rauf & Ashraf, 2009). In addition, the operations can be carried out under ambient temperature and pressure (Chong et al, 2010). Furthermore, this process can utilize sunlight as a renewable, high availability and economic light source, which is lower cost compared to processes involving ozone generation, electrodes or others which required high cost (Ahmed et al, 2010; Ribeiro et al, 2015).

2.4.1 Zinc Oxide as Photocatalyst

Zinc oxide (ZnO), which typically appears as white coloured powder is an oxidic compound. It has near insolubility in water. It is also optically transparent under visible range. At ambient conditions, the ZnO crystalized in a wurtzite structure. Figure 2.2 shows the stick and ball representation of the ZnO wurtzite structure (Lam et al, 2012; Raoufi, 2013):

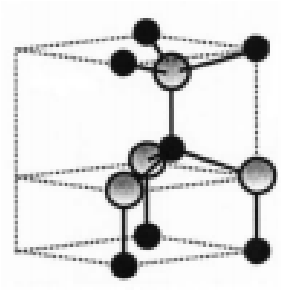

Figure 2.2: Stick and Ball Representation of the ZnO Wurtzite Structure. The Shaded Grey and Black Spheres Denote Zn and O Atoms, Respectively (Lam et al, 2012; Raoufi, 2013).

Since the photocatalyst is one of the main components in the photocatalytic reaction, it is important to make an appropriate catalyst selection. Examples of characteristics of an ideal catalyst are chemical and photostability, capability to adsorb reactants under efficient photonic activation, possess a band gap where oxidation potential of hydroxyl radicals and reduction potential of superoxide radical are within the gap, low cost and good availability. The band gab position of some common semiconductor is shown in Figure 2.3 (Lam et al, 2012; Ribeiro et al, 2015):

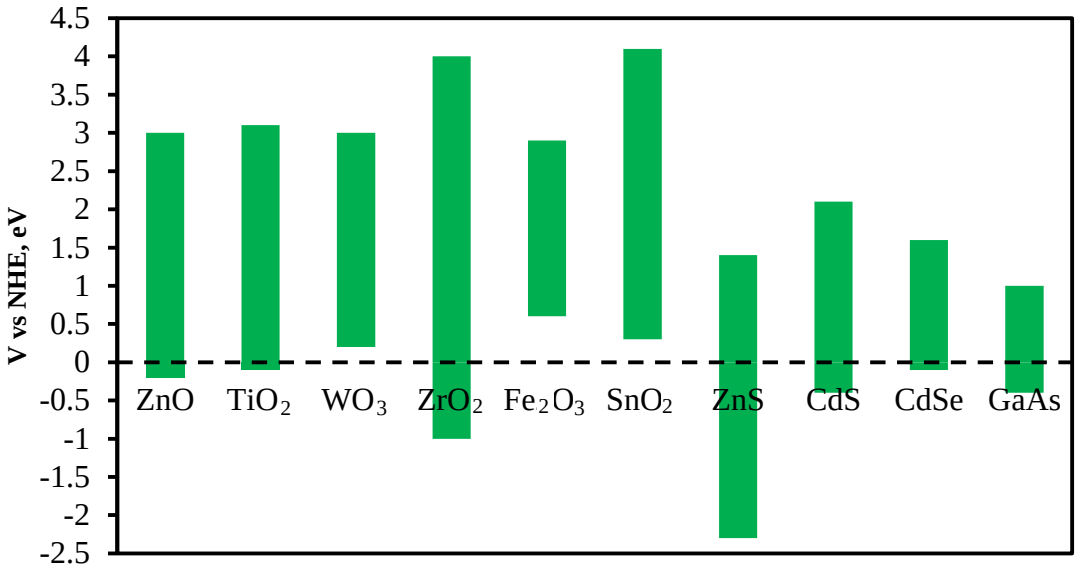

Figure 2.3: Band Gap Position of Some Common Semiconductors (Lam et al, 2012; Ribeiro et al, 2015).

The zinc oxide has been one of the most popular choices of photocatalyst because it has near ideal characteristics and has gained major attentions (Hariharan, 2006; Ribeiro et al, 2015). It has a wide band gap (3.37 eV) and has similar

photodegradation activity compared to the widely used TiO_2 catalyst as well as low cost (Chakrabarti & Dutta, 2004; Xie et al, 2011; Ribeiro et al, 2015). It also possesses excellent quantum efficiency and solar absorption capacity which lead to higher photocatalytic activity (Chakrabarti & Dutta, 2004; Xie et al, 2011). Some examples of organics that can be degraded by the ZnO photocatalyst are tabulated in Table 2.2.

Table 2.2: Examples of Organics that can be Degraded by the ZnO Photocatalyst

Class of Organics	Examples	References
Haloalkanes/haloalkenes	Chloroform, trichloroethylene	Hariharan (2006); Joo et al (2013)
Aliphatic carboxylic acids	Formic	Mrowetz & Selli (2006)
Aromatics	Toluene	Hariharan (2006)
Phenolic Compounds	Phenol	Ahmed et al (2010)
Halophenols	Chlorophenol	Hariharan (2006), Ahmed et al (2010)
Dyes	Methyl Orange, Reactive Blue 4, Naphthol Blue Black	Xu et al (2010); Krishnakumar et al (2014); Sanna et al (2015)

2.4.2 Mechanism of ZnO Photocatalysis

When the ZnO photocatalysts are illuminated by photons of higher or equal energy ($h\nu$) than the band gap (E_g) of the ZnO ($h\nu \geq E_g$), the absorption of the radiation and the photo-excitement of valence band electrons occurred. The excited electrons (e_{cb}^-) in the valence band are promoted to the conduction band. This leads to the formation of positive hole (h_{vb}^+) in the valance band and subsequently the generation of electron–hole pairs (e_{cb}^-- h_{vb}^+) (Rauf & Ashraf, 2009; Ahmed et al, 2010; Lam et al., 2012; Ribeiro et al, 2015). The mechanism of the formation of e_{cb}^-- h_{vb}^+ pairs is as follow (Equation 2.5):

$$ZnO + h\nu \rightarrow ZnO\ (e_{cb}^- + h_{vb}^+) \quad (2.5)$$

Both of the e_{cb}^- and h_{vb}^+ can then move to the catalyst's surface where they can initiate redox reaction with other species (Rauf & Ashraf, 2009; Ribeiro et al,

2015). The h_{vb}^+ are excellent oxidants which can lead to direct and indirect oxidation of adsorbate pollutant (R). In the direct oxidation process, the pollutants are oxidized by h_{vb}^+ (Equation 2.6). In the indirect oxidation process, the h_{vb}^+ can react with electron donors like water and hydroxyl ions (OH^-) to generate strong oxidizing •OH radicals (Equation 2.7-2.8) (Rauf & Ashraf, 2009; Ahmed et al, 2010; Lam et al, 2012; Ribeiro et al, 2015):

$$h_{vb}^+ + R_{ads} \rightarrow R_{ads}^+ \quad (2.6)$$

$$h_{vb}^+ + H_2O \rightarrow \bullet OH + H^+ \quad (2.7)$$

$$h_{vb}^+ + OH^- \rightarrow \bullet OH \quad (2.8)$$

As for the e_{cb}^-, they can be scavenged by electron acceptors in order to stop the recombination with the h_{vb}^+. The oxygen molecules (O_2) are one of the excellent electron acceptors and they can be reduced by the e_{cb}^- to form $O_2\bullet^-$ radicals (Equation 2.9). Subsequently, a series of further reactions could occur to provide an additional pathway of •OH radical generation (Equations 2.9-2.14). The generated active radicals can then degrade the organic pollutants into final products of CO_2 and H_2O (Equation 2.15) (Rauf & Ashraf, 2009; Ahmed et al, 2010; Lam et al, 2012):

$$e_{cb}^- + O_2 \rightarrow O_2\bullet^- \quad (2.9)$$

$$O_2\bullet^- + H^+ \rightarrow HO_2\bullet \quad (2.10)$$

$$2\ HO_2\bullet \rightarrow H_2O_2 + O_2 \quad (2.11)$$

$$H_2O_2 + O_2\bullet^- \rightarrow OH^- + \bullet OH + O_2 \quad (2.12)$$

$$H_2O_2 + e_{cb}^- \rightarrow OH^- + \bullet OH \quad (2.13)$$

$$H_2O_2 + h_{vb}^+ \rightarrow 2\bullet OH \quad (2.14)$$

Dye + (•OH, $HO_2\bullet$, $O_2\bullet^-$ or h_{vb}^+) → intermediates → final products (including CO_2 and H_2O) (2.15)

From the mechanisms above, it can be seen that the electron-hole pairs are very important in the photoatalytic reaction. However, the electron-hole pair recombination could also occur in the photocatalysis because of the competition with charge transfer to adsorbed pollutants. The recombination happens either in or on the photocatalyst surface together with dissipation of heat energy (Equation 2.16) (Chong et al, 2010; Lam et al, 2012).

$$e_{cb}^- + h_{vb}^+ \rightarrow ZnO + heat \quad (2.16)$$

Figure 2.4 shows the overall mechanism of the active species generation (Rauf & Ashraf, 2009):

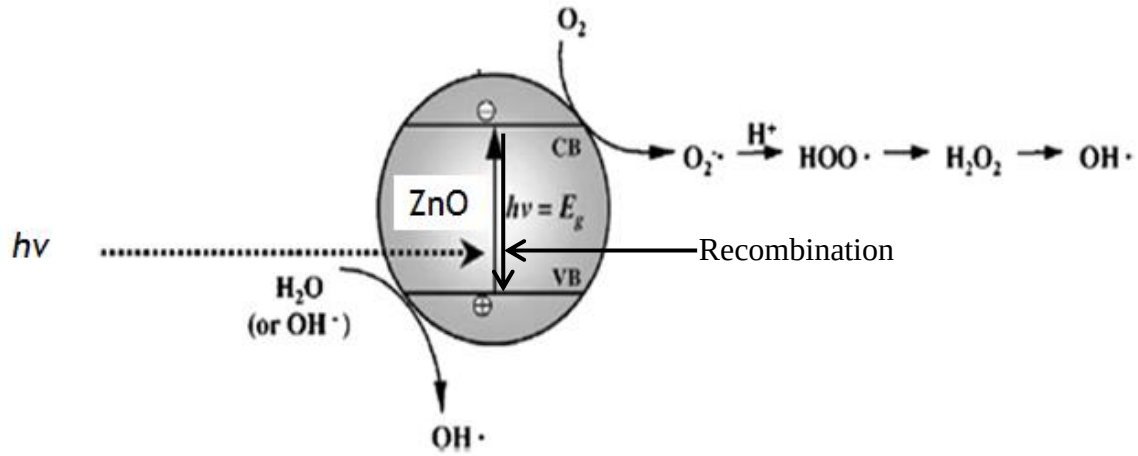

Figure 2.4: Schematic Diagram Displaying the Production of Oxidative Agents via Photocatalytic Reaction (Rauf & Ashraf, 2009).

2.5 Nanoscale ZnO

The nanoscale particles have distinct physical and chemical properties compared to the bulk materials (Hariharan, 2006). The properties of ZnO nanoparticles heavily relied on the microstructures of the materials such as the crystal size, morphology and crystalline density (Raoufi, 2013). For a semiconductor catalyst, the catalytic activity is expected to be increased due to the change in the surface area and surface properties (Hariharan, 2006). When the particle of the catalyst decreased to nanometers, the number of active sites for adsorption will be increased due to the higher surface-to-volume ratio as compared to the bulk material (Hariharan, 2006; Mekasuwandumrong et al, 2010).

There have been different methods in synthesizing nanoscale ZnO and they are principally classified into three types; vapour phase, solution, and solid. Examples of the synthesizing methods are vapour transport process, spray pyrolysis and drying, sol-gel processing, thermal decomposition, direct precipitation, homogeneous precipitation, hydrothermal synthesis, microemulsion synthesis, supercritical water processing, mechanochemical processing, sonochemical or microwaved assisted synthesis, laser ablation, electrochemical deposition, ultrasound, anodization, co-precipitation, electrophoretic deposition and etc (Hong et al, 2006; Kumar et al, 2013; Raoufi, 2013). A wide variety of nanostructured ZnO like nanoparticle, hollow sphere, nanobelt, nanorod, nanoplate, and micro/nanostructure, have been employed in the photodegradation of dye pollutants (Xie et al, 2011).

Hariharan (2006) has found out that the photocatalytic efficiency of nanoscale ZnO was higher compared to the bulk ZnO and commercial TiO_2 (Degussa-P25) in the degradation of 4-chlorophenol (Hariharan, 2006).

2.6 Photocatalytic Activiy of ZnO

ZnO photocatalyst has been able to degrade several types of dye effectively. The ZnO's photcatalytic activity on various dye pollutants under various conditions has been studied and summarised in Table 2.3.

Table 2.3: Photocatalytic Activity of ZnO on Various Dye Pollutants

Photocatalyst	Target Compound	Reaction Condition	Degradation Efficiency (%)	Reference
ZnO	Methyl Orange	Under a 300 W high pressure mercury lamp irradiation; Methyl Orange concentration = 10 mg/L; volume = 1L; catalyst loading = 2.5 g/L; solution pH = 7; irradiation time = 120 min	95	Chen et al (2011)
ZnO	Methylene Blue	Under 2 × 15 W UV tube irradiation; Methylene Blue concentration = 10 ppm; volume = 200 mL; catalyst loading = 100 mg/L; solution pH = 6.3; irradiation time = 60 min	70	Mekasuwandumrong et al (2010)
ZnO	Acid Blue 92	Under UV lamp irradiation; Acid Blue 92 concentration = 20 ppm; catalyst loading = 100 ppm; solution pH = 6; irradiation time = 120 min	100	Mohaghegh et al (2014)
ZnO	Acid Red 14	Under 30 W mercury lamp irradiation; Acid Red 14 concentration = 20 ppm; volume = 50 mL; catalyst loading = 160 ppm; solution pH = 7; irradiation time = 60 min	100	Daneshvar, Salari & Khataee (2004)

Table 2.3: Continued

Photocatalyst	Target Compound	Reaction Condition	Degradation Efficiency (%)	Reference
ZnO	Eosin Y	Under 16W UV lamp irradiation; Eosin Y concentration = 25 mg/L; volume = 400 mL; catalyst loading = 1 g/L; solution pH = 6.9; irradiation time = 120 min	90	Chakrabarti & Dutta (2004)
ZnO	Rhodamine B	Under 250 W high pressure mercury lamp irradiation; Rhodamine B concentration = 1×10^{-5} mol L^{-1}; volume = 100 ml; catalyst loading = 200 mg/L ; irradiation time = 50 min	77	Lai et al (2011)
ZnO annealed at 600˚C	Direct Red 23	Under 125 W low pressure mercury lamp irradiation; Direct Red 23 concentration = 40 ppm; volume = 150 mL; catalyst loading = 0.5 g/L; irradiation time = 80 min	97	Umar et al (2015)

2.7 Effects of Operating Parameter

There are several factors that can affect the photocatalytic degradation processes. Such factors are the nature of the catalyst and target pollutant, catalyst loading, concentration of pollutants, light intensity and wavelength, interfering species in solution media and solution pH (Lam et al, 2012; Ribeiro et al, 2015). In this literature review, three important factors which were initial pollutant concentration, solution pH and catalyst loading were chosen to be discussed.

2.7.1 Effect of Initial Dye Concentration

It was reported that the concentration of dye was proportional to the number of dye molecules get adsorbed on the photocatalyst's surface. When the concentration of dye was high, the amount of available active sites for the reaction between active radicals and dye molecules decreased because of the competitive adsorption of dye molecules on the ZnO surface. With constant light intensity and irradiation time, the number of active radicals formed on the catalyst surface was still the same. Thus, lesser active radicals in attacking the dye which led to lower degradation rate. Furthermore, the amount of light being absorbed by the dye molecules increased as the dye concentration increased. Thus, lesser photons reached to the catalyst surface and resulted a lower generation of active radicals to degrade the dye molecules. In addition, degradation of higher concentration dye effluent led to higher concentration of intermediates. These intermediates can adsorb on the surface of the catalyst and decreased the efficiency of photocatalytic degradation by competing with the parent molecules for the same active sites available on the photocatalyst surface (Ahmed et al, 2010; Lam et al, 2012).

Lam et al (2012) reviewed the effect of initial dye concentration on the photocatalytic degradation of methylene blue and eosin Y using ZnO nanoparticles. As the initial concentration of methylene blue increased from 25 to 100 mg/L, the degradation efficiency decreased from 87 to 40 %. As for the eosin Y, the degradation efficiency decreased from 93 to 63 % as the initial concentration of the solution increased from 25 to 50 mg/L. However, further increase in the concentration did not influence the degradation significantly. Velmurugan and Swaminathan (2011) investigated the effect of initial dye concentration on the

degradation of Reactive Red 120 using ZnO nanocrystals. When the initial concentration of dye increased from 1×10^{-4} to $4\times10^{-}4$ M, the degradation rate decreased from 0.173 to 0.012 min^{-1}. Other examples of the effect of initial dye concentration are tabulated in Table 2.3

Table 2.4: Effect of Initial Dye Concentration on the Photocatalytic Degradation of Various Dyes

Dye degraded	Photocatalyst	Tested initial dye concentration	Maximum degradation efficiency on tested initial dye concentration (%)	References
Acid dye				
Methyl Orange	ZnO	5-25 mg/L	86.6(5 mg/L)	Sanna et al (2015)
Naphthol Blue Black	ZrS_2 doped ZnO	20-50 ppm	60.4(20 ppm)	Krishnakumar et al (2014)
Acid Yellow 23	ZnO	20-50 mg/L	100.0(20 mg/L)	Modirshahla et al (2011)
Basic Dye				
Methylene Blue	W doped ZnO	1×10^{-5}- $3.5\times10^{-}5$ M	89.0($1\times10^{-}5$ M)	Moafi, Zanjanchi & Shojaie (2013)
Reactive dye				
Remazol Red RR	ZnO	50-250 mg/L	100.0(50 mg/L)	Akyol & Bayramoglu (2005)

2.7.2 Effect of Solution pH

The solution pH is another important factor in photocatalytic degradation. It can determine the surface charge properties of the catalyst and the size of aggregates it formed which subsequently affected the degradation rate (Gaya & Abdullah, 2008; Ahmed et al, 2010; Lam et al, 2012). Due to the amphoteric behaviour of ZnO particles, it can be protonated and deprotonated under acidic and alkaline conditions, respectively as shown in Equations 2.17 and 2.18 (Rauf & Ashraf, 2009; Lam et al, 2012):

$$\text{Protonation: } ZnOH + H^+ \rightarrow ZnOH_2^+ \quad (2.17)$$

$$\text{Deprotonation: } ZnOH + OH^- \rightarrow ZnO^- + H_2O \quad (2.18)$$

The pH of zero point charge (pH_{zpc}) of ZnO was estimated to be 9.3. Thus, the surface of the ZnO catalyst was expected to be protonated at a pH less than 9 and deprotonated at a pH above 9. Under the deprotonated state, there will be many OH^- ions on the ZnO catalyst surface and in the solution. The catalyst surface will become negatively charged due to the adsorbed OH^- ions. With the presence of large amount of OH^- which can react with holes to form the •OH radicals, the photocatalytic activity is anticipated to be improved. However, the degradation rate is lower in some cases because of the electrostatic repulsion between the OH^- ions and the negatively charged ZnO surface in alkaline solution which resulted in slower production of •OH radicals (Lam et al, 2012). The organic compounds in the dye effluent also have different parameters such as speciation behaviour, hydrophobicity, and solubility in water and the variation of such parameters may be great. Although some dyes remained uncharged at typical wastewater pH, others may show a wide variation in speciation (or charge) and physic-chemical properties. The interaction and affinity between the catalyst and the dye pollutants will heavily depend on these characteristics when there is a variation of solution pH (Ahmed et al, 2010; Lam et al, 2012).

Lam et al. (2012) reviewed the effect of pH on the photocatalytic degradation of C.I Reactive Red 198 in the presence of ZnO and UV light. After 120 minutes of irradiation, the degradation rate constants at pH 4, 7 and 10 were found to be 0.0116, 0.0534 and 0.0637 min^{-1}. Velmurugan and Swaminathan (2011) have investigated the effect of pH on the photocatalytic degradation of Reactive Red120 using ZnO under solar light irradiation. The range of the pH was from 3 to 11 and pH at 5 was

found to have higher degradation rate than the alkaline solution. This was due to the high adsorption rate of the dye pollutant onto the positively charge catalyst surface. In short, different catalysts and dye pollutants will exhibit different activities at different pH values. The degradation rate will be dependent on the nature of the photocatalyst and dye pollutants. Thus, it is essential to study the behaviour of the target dye pollutants so as to determine the optimum pH value for the photocatalytic degradation process. Other examples of the effect of solution pH are tabulated in Table 2.4.

Table 2.5: Effect of Solution pH on the Photocatalytic Degradation of Various Dyes

Dye degraded	Photocatalyst	Range of solution pH	Optimum solution pH	Degradation/mineralization efficiency	References
Acid dye					
Acid Brown 14	ZnO	3.0-11.0	10.0	$2.58 \times 10^{4}\ s^{-1}$	Sakthivel et al (2002)
Biebrich Scarlet	ZnO	3.0-11.0	10.0	100 %	Kansal, Kaur & Singh (2009)
Acid Red 14	ZnO	4.0-12.0	7.0	100 %	Daneshwar, Salari & Khataee (2004)
Methyl Red	ZnO	2.0-12.0	6.0	~80 %	Comparelli et al (2005)
Methyl Orange	ZnO	2.0-12.0	6.0	~60 %	Comparelli et al (2005)
Basic Dye					
Rhodamine B	ZnO	4.5-10.5	7.0	100 %	Zhai et al (2010)

Table 2.5: Continued

Dye degraded	Photocatalyst	Range of solution pH	Optimum solution pH	Degradation/mineralization efficiency	References
Reactive Dye					
Reactive Black 5	ZnO	3.0-11.0	4.0	100 %	Kansal, Hassan & Kapoor (2010)
Reactive Orange 4	ZnO	3.0-11.0	11.0	100 %	Kansal, Hassan & Kapoor (2010)
Direct Dye					
Direct Yellow 12	ZnO	4.0-10.0	10.0	1.4 μM min^{-1}	Rao, Sivasankar & Sadasivam (2009)
Mordant Dye					
Alizarin Yellow GG	ZnO	5.0-12.2	5.0	~80 %	Hayat et al (2010)

2.7.3 Effect of Photocatalyst Loading

The increase in the photocatalyst loading is able to improve the degradation efficiency due to the larger amount of active surface area of catalyst as well as higher light absorption. The increase of active surface area means more active sites for carrying out the photocatalytic reactions. In addition, more catalysts are exposed to the light so the amount of photo being absorbed increased. Thus, the degradation efficiency will be enhanced. However, when the catalyst loading exceeded a certain amount, the light penetration will be decreased because of the increased amount of suspension. When the turbidity increased, light scattering occurred and led to lesser effective photoactivated volume of suspension. Another problem with overloaded catalyst loading is the occurrence of aggregation. When the particles aggregated, not all surfaces are exposed to the light irradiation. Thus, the photons absorption will not increase in geometric ratio. So, increasing the catalyst does not necessary means a linear increase in degradation rate (Ahmed et al, 2010; Lam et al, 2012). With these two phenomena clashing with each other, many studies indicated that there existed an optimum catalyst loading for the photocatalytic degradation (Ahmed et al, 2010; Lam et al, 2012; Ribeiro et al, 2015).

Sakthivel et al (2002) studied the optimum ZnO catalyst loading on the photocatalytic degradation of Acid Brown 14 dye. With the presence of solar light, the rate of degradation increased from 0.88×10^{4} to 2.48×104 s^{-1} as the catalyst concentration increased up to 2.5 g/L. Beyond that concentration, the turbidity restricted the photons absorption. Nishio et al (2006) have investigated the effect of ZnO catalyst loading on the photocatalytic degradation of Orange II. As the ZnO concentration increased up to 1,000 mg/L, the degradation rate constant increased rapidly. After the concentration increased beyond 1,500 mg/L, the rate constant remained the same. Other examples of effect of catalyst loading on the photocatalytic degradation of other dyes are tabulated in Table 2.5

Table 2.6: Effect of Catalyst Loading on the Photocatalytic Degradation of Various Dyes

Dye degraded	Photocatalyst	Tested catalyst concentration (g/L)	Optimum catalyst concentration	Degradation/mineralization efficiency	References
Acid dye					
Eosin Y	ZnO	0.5-5.0	2.5	74 %	Chakrabarti & Dutta, (2004)
C.I Acid Orange 7	ZnO	0.1-0.2	0.16	~98 %	Daneshvar et al (2007)
Basic Dye					
Rhodamine B	ZnO	1.0-8.0	6.0	0.045 min^{-1}	Byrappa et al (2006)
Methylene Blue	ZnO	1.0-10.0	6.0	76 %	Chakrabarti & Dutta, (2004)
Reactive Dye					
Reactive Red 120	ZnO	2.0-6.0	4.0	0.048 min^{-1}	Velmurugan & Swaminathan (2011)
Reactive Blue 4	ZnO/sepiolite	0.1-0.5	0.5	100 %	Xu et al (2010)

Table 2.6: Continued

Dye degraded	Photocatalyst	Tested catalyst concentration (g/L)	Optimum catalyst concentration	Degradation/mineralization efficiency	References
Direct Dye					
Direct Yellow 12	ZnO	1.0-5.0	4.0	1.1 μM min^{-1}	Rao, Sivasankar & Sadasivam (2009)
Congo red	ZnO	0.025-0.25	0.16	97 %	Annadurai, Sivakumar & Rajesh Babu (2000)
Mordant Dye					
Alizarin Yellow GG	ZnO	1.0-4.0	3.0	~0.070 min^{-1}	Hayat et al (2010)

CHAPTER 3

METHODOLOGY

3.1 Overall Flowchart of the Work

This study comprises of several experimental steps. Figure 3.1 summarized the overall steps that are carried out in this study:

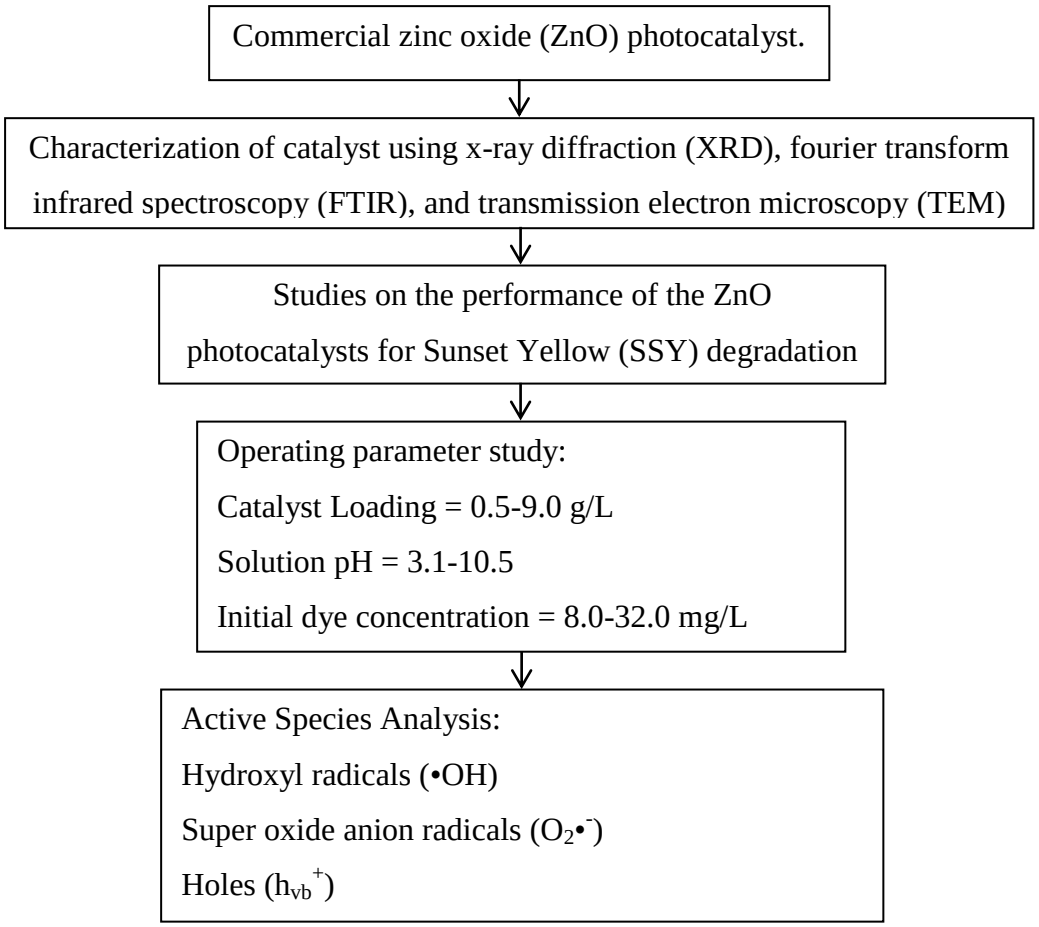

Figure 3.1: Flow Chart of the Overall Methodology

3.2 Materials and Chemicals

Table 3.1 summarized the chemicals and Materials used in the experiment.

Table 3.1: List of Chemical and Materials

Chemical/material	Purity	Supplier	Application
1,4-Benzoquinone ($C_6H_4O_2$)	98 %	Acros Organics	Active species analysis
Distilled water		Gainson Advanced Technology	Dye solution and pH adjustors preparation
Absolute Ethanol (C_2H_6O)	99.9 %	Chem Sol	Active species analysis
Sodium Hydroxide (NaOH)	≥ 96 %	Uni-Chem Chemical Reagents	pH adjustment
Sodium Oxalate ($Na_2C_2O_4$)	≥ 99.9 %	Univar	Active species analysis
Sulfuric Acid (H_2SO_4)	95-97 %	QRëC	pH adjustment
Sunset Yellow FCF ($C_{16}H_{10}N_2Na_2O_7S_2$)	> 90 %	Tokyo Chemical Industry	Model dye pollutant
Zinc Oxide (ZnO)	≥ 99.5 %	Acros Organics	Photocatalyst

3.3 Photocatalytic Degradation Experiment Setup

The laboratory experiment setup consisted of a batch reaction system. The photocatalytic degradation experiments were carried out in a beaker with a volume of 250 mL. The light source for the experiments was a 45 W fluorescent lamp supplied by Universal. It was placed 16 cm above the dye solution. The light intensity irradiated on the dye solution surface was 2500 lx. The beaker was placed on a hot plate stirrer supplied by Fisher Scientific for agitation so as to ensure a homogeneous mixing of photocatalyst. The lamp, beaker and the stirrer were placed inside an acrylic black box in order to prevent any stray light from entering the reaction system. An air pump supplied by Sobo was used to supply air into the dye solution throughout the experiment. The amount of air entering the system was controlled by a flow meter supplied by Dwyer. Apart from that, cooling blower fans supplied by

Toyo were used for cooling purpose. Figure 3.2 shows the schematic diagram of the photoatalytic degradation laboratory experiment setup.

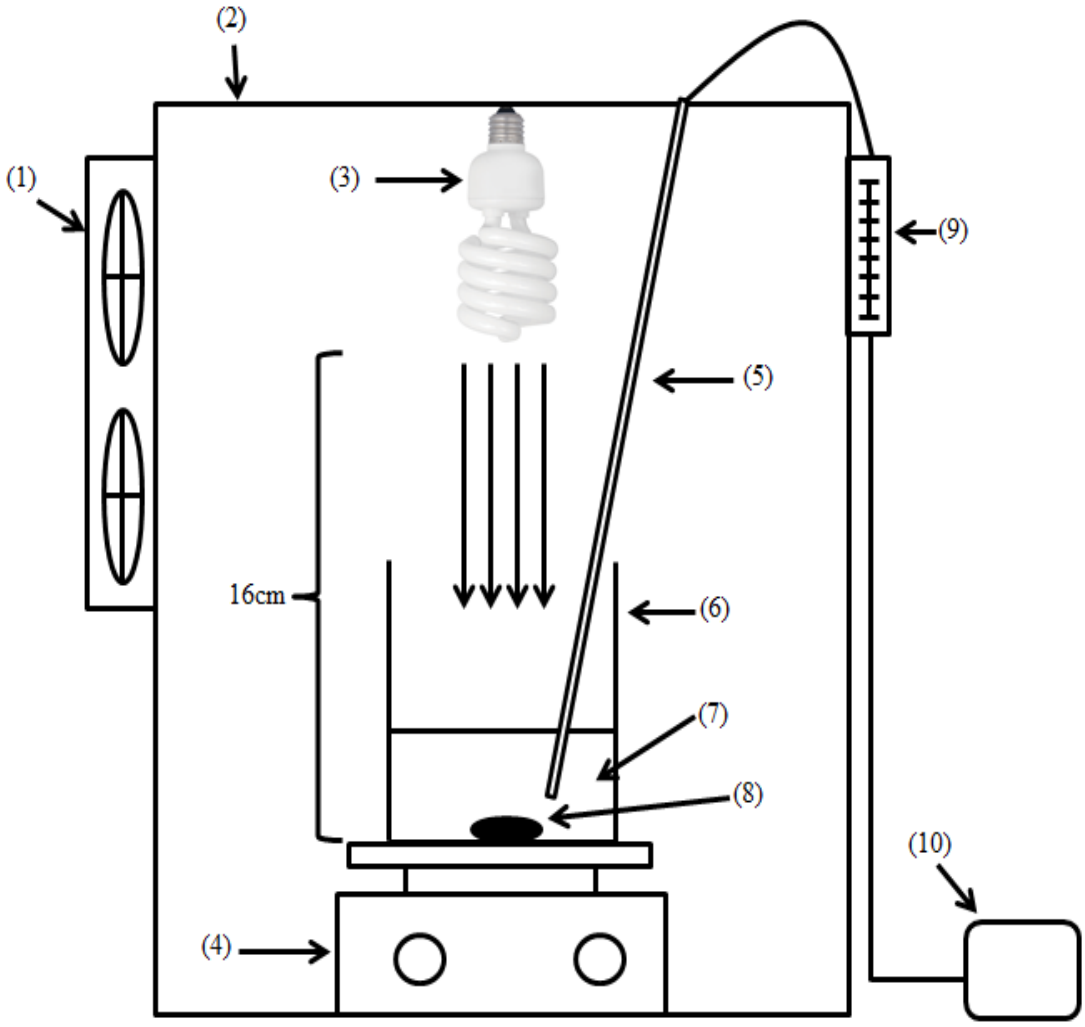

Figure 3.2: Schematic Diagram of the Photocatalytic Degradation Reaction System under Irradiation of Fluorescent Light. (1) Cooling Blower Fans, (2) Acrylic Black Box, (3) Fluorescent Lamp, (4) Hot plate Stirrer, (5) Air Supply,(6) Beaker, (7) Dye Solution, (8) Magnetic bar, (9) Flow Meter, (10) Air Pump.

3.4 Characterization

The crystal phase of the ZnO photocatalysts was analysed by a X-ray diffraction (XRD) using XRD-6000 supplied by Shimadzu. Surface morphology and particle size analysis of the ZnO samples were carried out using a transmission electron microscopy (TEM) supplied by Philips. The functional groups of the samples were performed via a fourier transform infrared spectroscopy (FTIR) using Spectrum RX 1 supplied by Perkin Elmer.

3.5 Photocatalytic Activity

In this study, the Sunset Yellow was used as the model pollutant to study the photocatalytic performance of the ZnO photocatalysts. The photocatalytic reaction of the photocatalysts was carried out in batch reaction system under fluorescent light. Before the beginning of the experiment, a SSY dye stock solution with concentration of 1000 mg/L was prepared by mixing the SSY powder with distilled water. At the beginning of an experimental run, the 100 ml substrate solution of certain concentration was prepared by mixing the right volume of SSY dye stock solution and distilled water. The prepared 100 mL substrate solution and certain amount of photocatalyst were fed into a beaker. Air was bubbled into the solution at a constant flow rate of 2.5 L/min during all experimental runs. A hot plate stirrer was used to continuously agitate the suspensions with the help of a magnetic stirrer and the stirring rate was 350 rpm for all experimental runs. Before photocatalytic reaction, the heterogeneous mixture was premixed in the dark for 30 minutes so as to achieve adsorption–desorption equilibrium of pollutant on the catalyst surface. Next, the solution was exposed to light irradiation. After the elapse of a period of time, 4 mL of the solution was withdrawn from the system and filtered with 0.45 μm syringe filters supplied by Whatman. After that, the sample was analysed by uv-vis spectrophotometer (Model: DR 6000) supplied by Hach. The spectrophotometer was also calibrated by using different concentration of SSY solutions to obtain the relation between the peak area and their concentrations. The uv-vis spectrophotometer calibration line for SSY concentration versus peak area is shown in Appendix A. The photocatalytic degradation efficiency was calculated as in equation (3.1):

$$\text{Dye degradation (\%)} = \frac{C_o - C_t}{C_o} \times 100\ \% \tag{3.1}$$

Where C_o was the concentration of dye after 30 min of dark run and C_t was the concentration of dye at reaction time, t (min).

3.5.1 Effect of Initial Dye Concentration

The effect of initial dye concentration on the photocatalytic degradation of SSY dye over the ZnO photocatalysts under fluorescent light irradiation was studied in the dye concentration range of 8.0 to 32.0 mg/L. The range was chosen based on literatures (Yang et al, 2010; Sanna et al, 2015). The initial dye concentration was adjusted by varying the volume of SSY dye stock solution and distilled water used to make the dye solution. The experiment runs were carried out with catalyst loading of 1 g/L and solution pH of 5.8.

3.5.2 Effect of Catalyst Loading

The effect of catalyst loading on the photocatalytic degradation of SSY dye over the ZnO photocatalysts under fluorescent light irradiation was studied in the loading range of 0.5 to 9.0 g/L. The range was chosen based on literatures (Chakrabarti & Dutta, 2004; Byrappa et al, 2006; Velmurugan & Swaminathan, 2011). The loading can be adjusted by controlling the amount of catalyst being fed into the reactor. The experiment runs were carried out with initial SSY concentration of 8 mg/L and solution pH of 5.8.

3.5.3 Effect of Solution pH

The effect of solution pH on the photocatalytic degradation of SSY dye over the ZnO photocatalysts under fluorescent light irradiation was studied in the pH range of 3.1 to 10.5. The pH was adjusted by the addition of 1 M H_2SO_4 or NaOH solution before irradiation. The pH adjustors were prepared by diluting the corresponding acid and alkaline with distilled water. The values of solution pH were chosen based on the different conditions such as acidic, natural, neutral and alkaline media. The experiment runs were carried out with initial SSY concentration of 8 mg/L and catalyst loading of 7 g/L.

3.5.4 Scavenger Test

The scavenger test was carried out in order to determine the active species that played the prominent role in the photocatalytic degradation of SSY dye over the ZnO

photocatalysts under fluorescent light irradiation. The reaction was carried out in a manner similar to the photocatalytic experiment (Section 3.5) except under the presence of different radical scavenger such as ethanol, 1,4-benzoquinone and sodium oxalate. The ethanol, 1,4-benzoquinone and sodium oxalate can act as the scavenger for •OH radicals , O_2•$^-$ radicals and h_{vb}^+ respectively (Daneshvar, Salari & Khataee, 2004; Jin et al, 2004; Misiaszek et al, 2004; Pelaez et al, 2012; Yang et al, 2013; Xian et al, 2014; Wang et al, 2015).The dosage of the radical scavenger for each run was 2 mM. The experiment runs were carried out with initial SSY concentration of 8 mg/L, catalyst loading of 7 g/L and solution pH of 5.8.

CHAPTER 4

RESULTS AND DISCUSSIONS

4.1 Characterization

Characterization tests were carried out on the ZnO photocatalyst so as to describe its features. The tests were fourier transform infrared (FTIR), X-ray diffraction (XRD), and transmission electron microscopy (TEM).

4.1.1 Fourier Transform Infrared (FTIR)

The FTIR characterization was carried out to analyse the functional group of ZnO photocatalyst as shown in Figure 4.1. The ZnO spectrum was dominated by the band of 478 cm^{-1} and 544 cm^{-1} which can be ascribed to the stretching of Zn-O bond (Wahab et al, 2007; Matei et al, 2008). Moreover, the broad absorption band at 3401 cm^{-1} and 1544 cm^{-1} band could be corresponded to the –OH groups and H_2O molecules strongly bound to the catalyst surface (Xiong et al, 2006; Wahab et al, 2007). The peaks at 874 cm^{-1} and 992 cm^{-1} could be due to the presence of impurities like alkenes. The results were also similar to other literatures (Hong, Qian & Cao, 2006; Wahab et al, 2007; Long et al, 2008; Matei et al, 2008; Azizi et al, 2014).

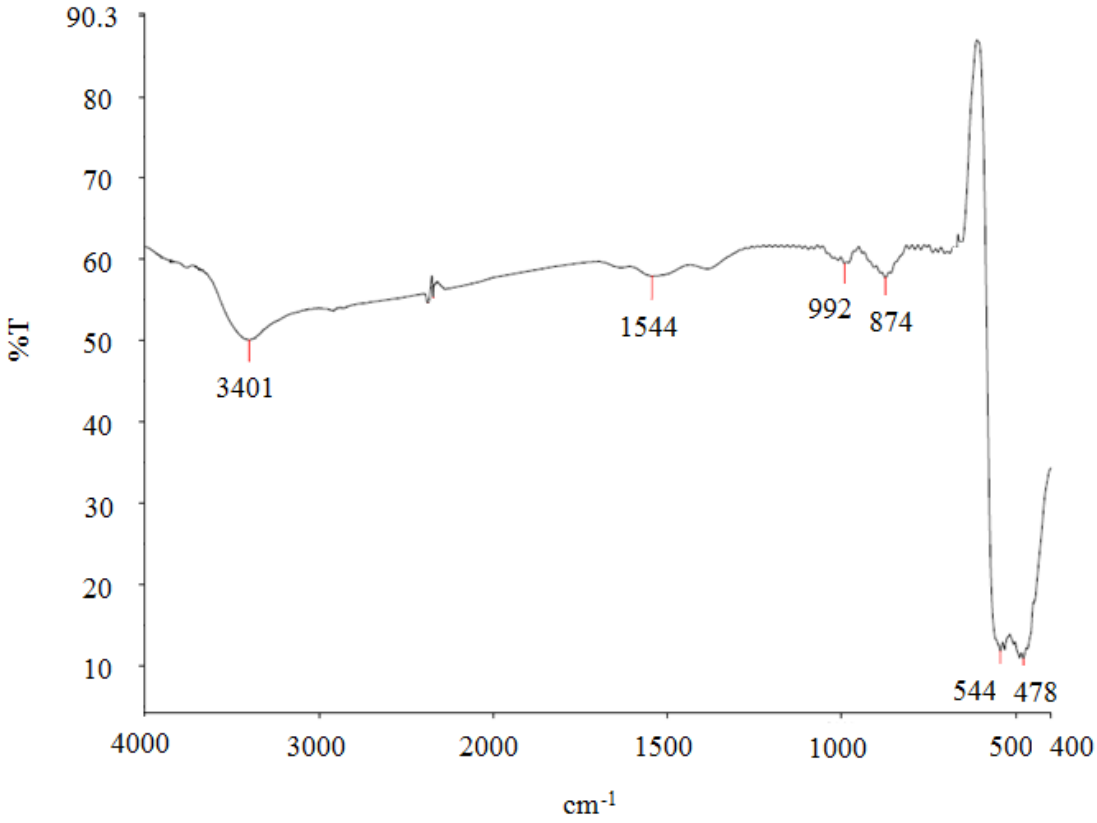

Figure 4.1: FTIR Spectrum of ZnO Photocatalysts

4.1.2 X-ray Diffraction (XRD)

The XRD characterization was performed to show the crystalline structure of the ZnO photocatalysts. Figure 4.2 shows the XRD pattern of the ZnO photocatalysts. All the diffraction peaks were labelled and can be readily indexed to hexagonal wurzite ZnO structure. The 2Θ of 31.821, 34.4651, 36.2886, 47.5941, 56.6508, 62.9114, 66.4064, 67.9868, 69.1113, 72.6063 and 76.9826 corresponded to the peaks (100), (002), (101), (102), (110), (103), (200), (112), (201), (004) and (202) respectively. No other crystalline impurities were detected in the pattern, indicating the phase purity of ZnO photocatalysts. The observed peaks were also similar to the results of several literatures (Seyed-Dorraji, Daneshvar & Aber, 2009;Yang et al, 2009; Dutta & Ganguly, 2012; Rahman et al, 2013; Pal, Sarkar & Giri, 2015; Vijayaprasath et al, 2016).

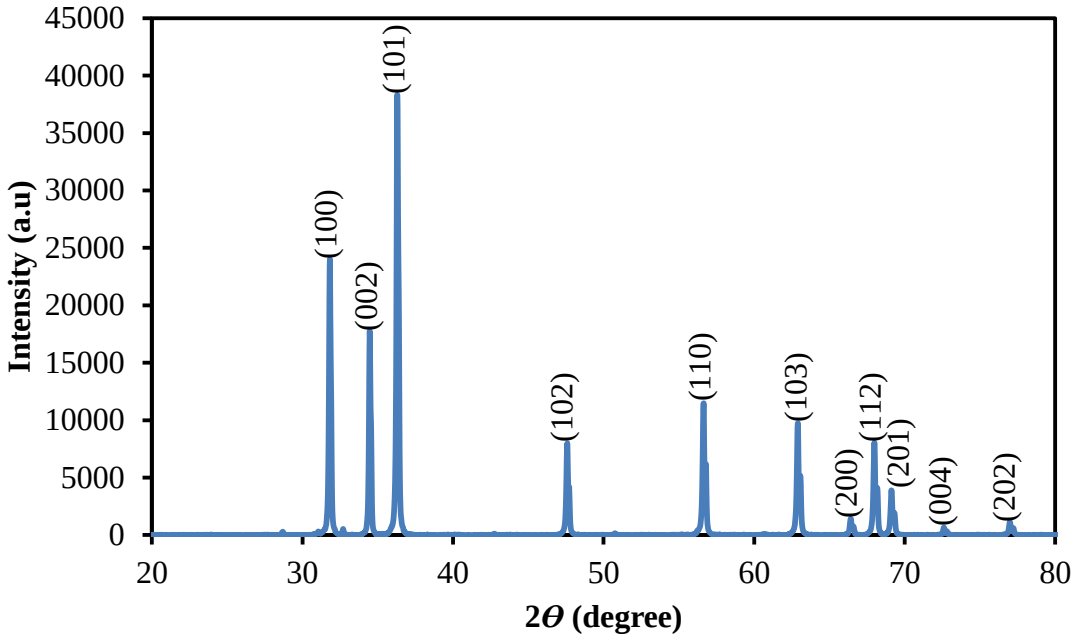

Figure 4.2: XRD Pattern of ZnO Photocatalysts

4.1.3 Transmission Electron Microscopy (TEM)

The TEM characterization was done to observe the morphology and particle size of the ZnO photcatalysts. Figure 4.3 shows the TEM image of ZnO nanoparticles. From the TEM image, the ZnO nanoparticles were identified in irregular shape. The particle sizes were measured to be in the range of 153 nm to 283 nm.

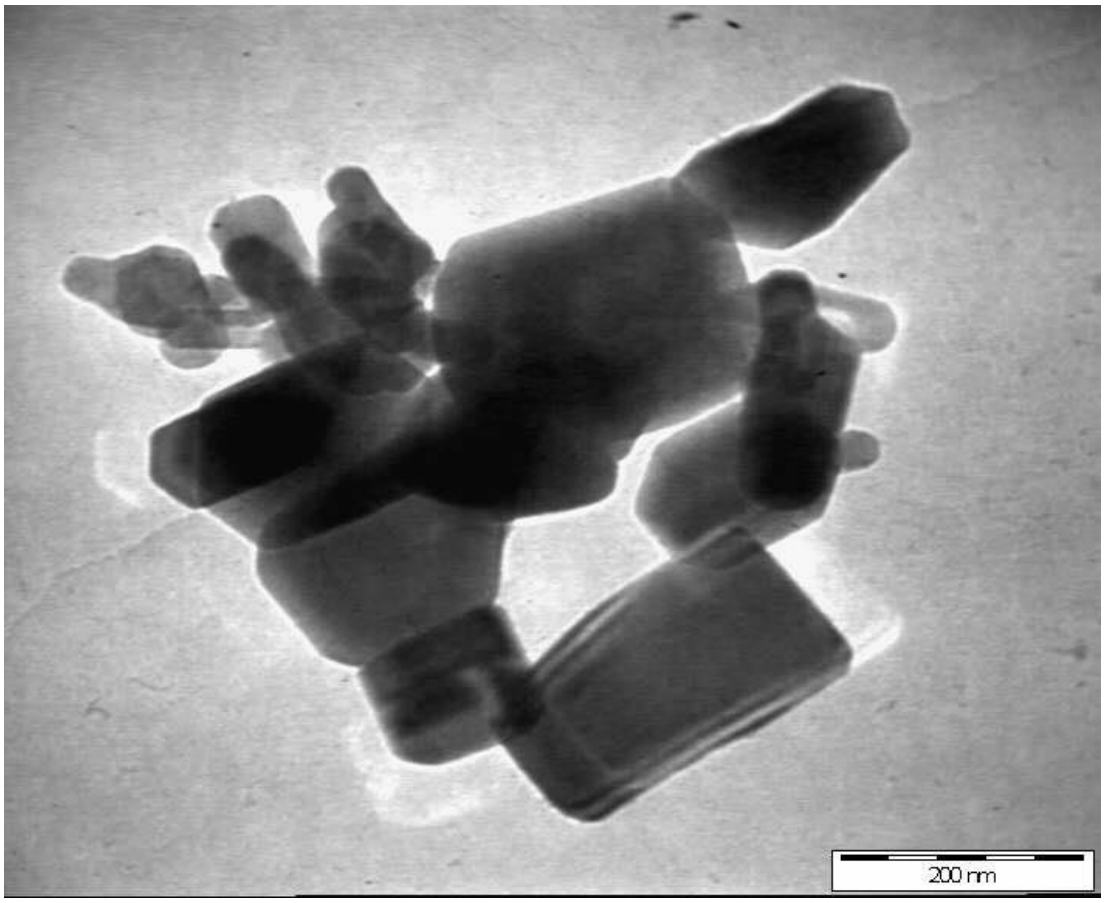

Figure 4.3: TEM Image of ZnO Nanoparticles

4.2 Control Experiment

The control experiments were carried out to show that the photocatalysis has took place in the presence of both light and catalyst. Thus, the effect of the presence of light and ZnO photocatalysts on the photocatalytic degradation of SSY was carried out with initial SSY concentration of 8 mg/L, ZnO catalyst loading of 1g/L and solution pH of 5.8. The dark run was also carried out with the presence of catalyst but without light irradiation to observe the catalyst adsorption. In addition, the photolysis run was carried out without the presence of catalyst but with light irradiation. The photocatalysis run was carried out with the presence of catalyst and light irradiation. Figure 4.4 shows the degradation efficiency of SSY under different conditions.

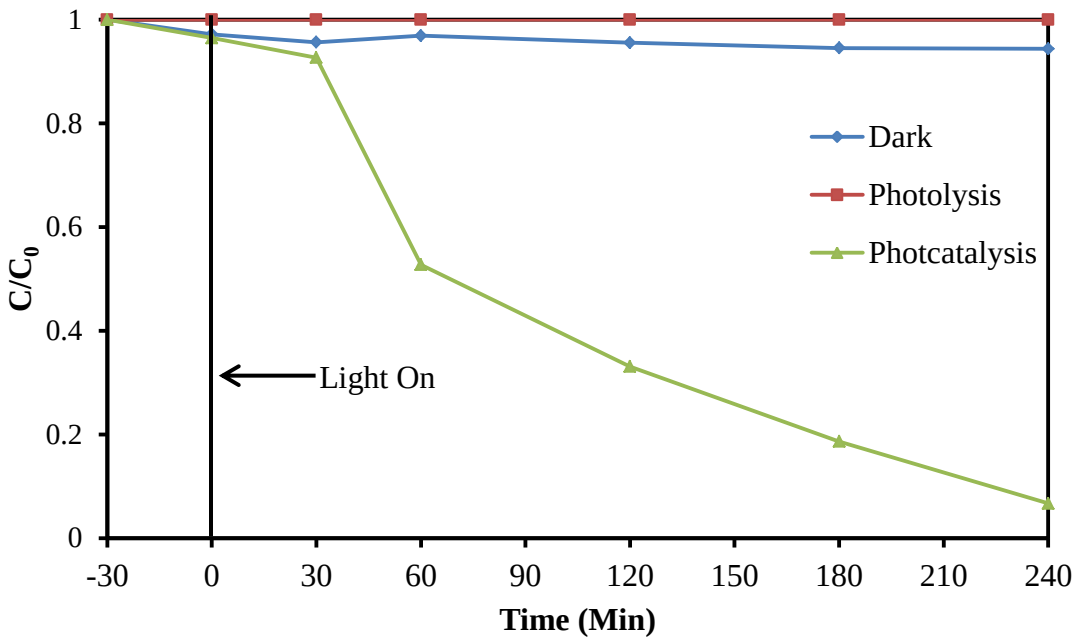

Figure 4.4: Photocatalytic degradation of SSY under different conditions. Conditions: Initial SSY Concentration = 8 mg/L, ZnO Catalyst Loading = 1 g/L, Solution pH = 5.8.

From the data, the degradation efficiency was very low for both dark and photolysis runs compared to the photocatalysis run. The photolysis run has negligible degradation. This was consistent with the report of Rajamanickam, Dhatshanamurthi, & Shanthi (2015). Rajamanickam, Dhatshanamurthi, & Shanthi (2015) have studied the photolysis of SSY dye under solar light irradiation. It was found that the degradation rate was only 0.3 % (Rajamanickam, Dhatshanamurthi, & Shanthi, 2015).

As for the dark run, it also has low degradation efficiency of 5.6 %. The concentration of SSY decreased slightly for the dark run due to the adsorption of dye molecules on the catalyst surface. The trend was similar to the findings of Mohsin, Juda, & Mashkour, (2013). They have carried out the dark adsorption experiment of SSY dye over ZnO photocatalysts. They reported that the degradation efficiency was 8.53 % after 35 min. Their results also confirmed that the decrease in SSY dye concentration was due to the adsorption of SSY dye molecules on the ZnO catalyst and there was no degradation of dye solution (Mohsin, Juda, & Mashkour, 2013).

However, the photocatalysis run accelerate the SSY degradation (93.3% degradation efficiency). It was well established that the photocatalytic degradation of organic matters in solution was initiated by the photoexcitation of semiconductors. With both light and catalyst, electron-holes pairs can be generated and it will lead to the formation of oxidizing agents for the degradation of organic pollutants. Thus, high degradation efficiency of SSY was observed in the presence of light and catalysts. In addition, comparing the results of photolysis, adsorption and photocatalysis, this indicated that the SSY degradation experiments were carried out at a nearly pure photocatalytic condition (Daneshvar, Salari & Khataee , 2004; Rauf & Ashraf, 2009; Ahmed et al, 2010; Lam et al, 2012; Ribeiro et al, 2015).

4.3 Effect of Operating Parameters

4.3.1 Effect of Initial Dye Concentration

The effect of initial SSY concentration was studied over ZnO photocatalysts under fluorescent light irradiation at constant catalyst loading and solution pH. The tested initial SSY concentrations were 8 mg/L, 16 mg/L, 24 mg/L and 32 mg/L in the presence of 1.0g/L ZnO and solution pH of 5.8. Figure 4.5 shows the degradation efficiency of SSY as a function of initial SSY concentration.

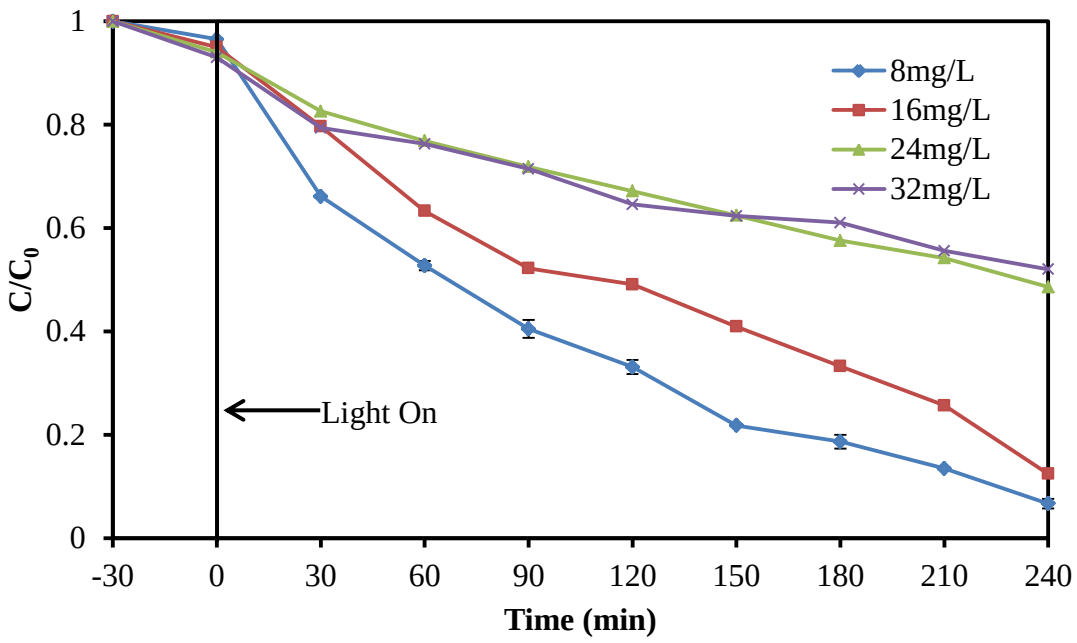

Figure 4.5: Effect of Initial SSY Concentration on the Photocatalytic Degradation of SSY over ZnO photocatalysts. Conditions: Catalyst Loading = 1 g/L, Solution pH = 5.8.

From the result, the degradation efficiency of SSY decreased as the initial SSY concentration increased. The degradation efficiency of SSY determined at lower initial SSY concentration of 8 mg/L (93.3 %) was much higher than those determined at 16 mg/L (87.6 %), 24 mg/L (51.4 %) and 32 mg/L (48.0 %). This trend of the result was also similar to the findings of Sanna et al (2015) and Modirshahla et al (2011). Sanna et al (2015) degraded the methyl orange dye using ZnO photocatalyst and found out that the degradation efficiency decreased from 86.6 % to 53.6 % as the initial dye concentration increased from 5 mg/L to 25 mg/L. Modirshahla et al (2011) have reported that the degradation efficiency of acid yellow 23 using ZnO photocatalysts decreased from 100.0 % to 46.0 % with the increase of initial dye concentration from 20 mg/L to 50 mg/L (Modirshahla et al, 2011; Sanna et al, 2015).

The decrease in the degradation efficiency at high concentrations could be due to the dye solution became more and more dense which can hinder the light from reaching the catalyst surface. Thus, lesser photon can reach the catalyst surface

which can result in lesser generation of active radicals to degrade the dye. At high concentration of SSY, the increased amount of SSY can also increase the adsorption of SSY molecules onto the catalyst surface. Since the number of active radicals generated on the catalyst surface did not increase under the constant light intensity and irradiation time, there will be lesser active radicals to attack the dye molecules and led to lower degradation efficiency. Furthermore, the concentration of intermediates also increased with increasing dye concentration. When the radicals attacked the dye molecules at high concentrations, a lot of intermediates can be generated. These intermediates can compete with the parent molecules for the limited active sites on the catalyst surface (Ahmed et al, 2010; Lam et al, 2012).

4.3.2 Effect of Catalyst Loading

It was known that catalyst loading has an effect on the photocatalytic degradation of organic pollutants. Thus, the effect of catalyst loading on the photocatalytic degradation of SSY over ZnO photocatalysts under fluorescent light irradiation was studied by varying the catalyst loading from 0.5 to 9 g/L at constant initial SSY concentration (8 mg/L) and solution pH (5.8). Figure 4.6 shows the degradation efficiency of SSY as a function of ZnO catalyst loading. After 180 min of irradiation, the degradation efficiency of SSY increased from 63.6 % to 100 % with increasing the catalyst loading from 0.5 to 7 g/L. However, at higher catalyst loading of 9 g/L, the degradation efficiency of SSY decreased to 97.59 %.

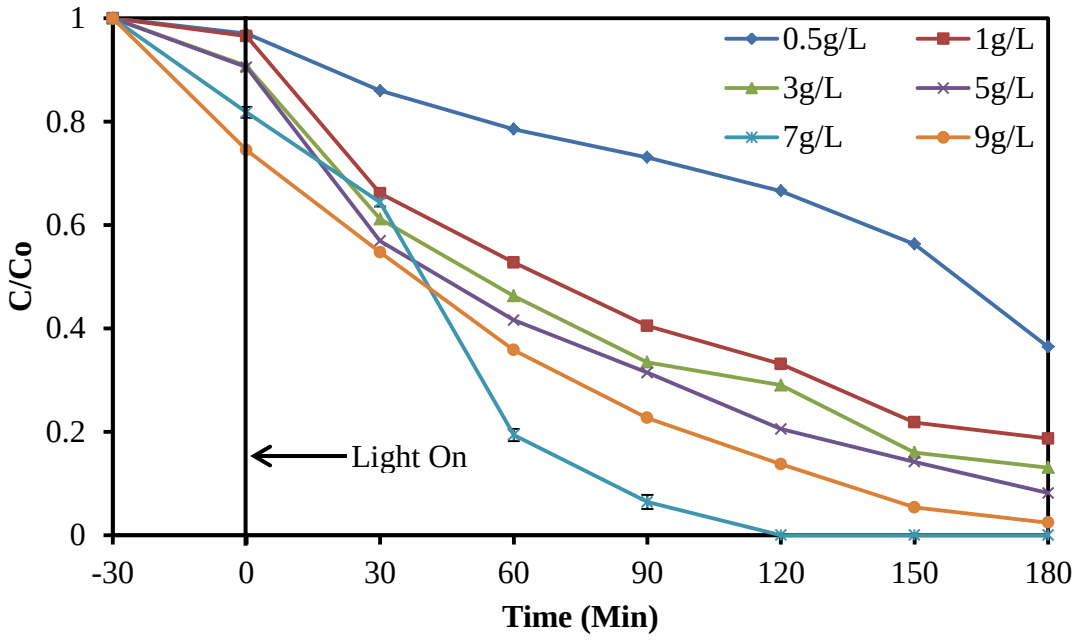

Figure 4.6: Effect of Photocatalysts Catalyst Loading on the Photocatalytic Degradation of SSY over ZnO. Conditions: Initial SSY Concentration = 8 mg/L, Solution pH = 5.8.

The effect of catalyst loading on the SSY degradation can be explained as the amount of catalyst increased, more catalyst active sites and higher adsorption area were available for the generation of active radicals to degrade the dye (Ahmed et al, 2010; Lam et al, 2012). Chen et al (2011) carried out the photocatalytic degradation of methyl orange in aqueous suspension of ZnO. They reported that the degradation efficiency increased as the ZnO loading increased to an optimum loading of 2.5 g/L due to the increased active surface area of the ZnO nanoparticles. However, increasing the catalyst loading beyond a certain amount can lead to lower degradation efficiency because of the light scattering effect and increase in the particle aggregation. Daneshvar et al (2007) also found the similar observation on the photocatalytic degradation of C.I Orange 7 using ZnO photocatalysts. They reported that the excess of catalyst led to an increase in the turbidity of the suspension and consequently increased the light scattering effect. Thus, the light penetration decreased which resulted in lower degradation efficiency (Daneshvar et al, 2007; Chen et al, 2011).

Generally, the optimum catalyst loading for ZnO-based photocatalysts was reported to be 0.16 g/L to 10.0 g/L from various studies which was dependent on the nature of photocatalyst, pollutants, light source and reactor configuration (Jiang et al, 2008; Lam et al, 2012; Rao et al, 2012). In conclusion, based on the results obtained, optimum ZnO loading was 7.0 g/L.

4.3.3 Effect of pH

The influence of solution pH on the photocatalytic degradation of SSY over ZnO photocatalysts under fluorescent light irradiation are shown in Figure 4.7. The inset shows the complete degradation of SSY dye under optimised operation parameters in 120 min. The initial pH of SSY solution was varied from 3.1 to 10.5 by using 1M H_2SO_4 and NaOH solutions. Here pH 5.8 was the pH value of SSY in distilled water without using pH adjustors. All experiments were carried out with initial SSY concentration of 8mg/L and catalyst loading of 7 g/L.

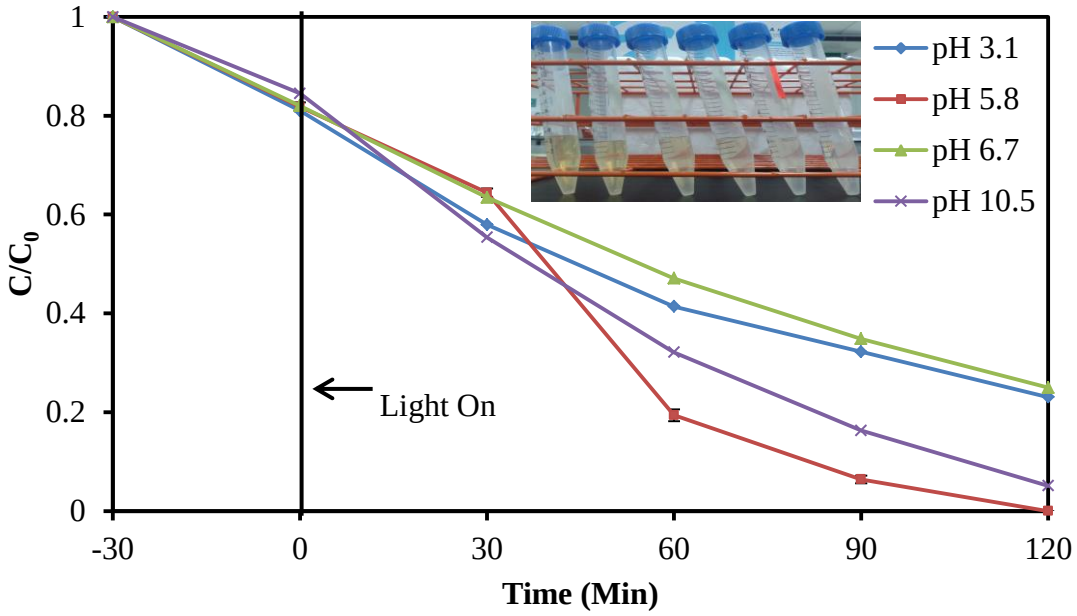

Figure 4.7: Effect of Solution pH on the Photocatalytic Degradation of SSY over ZnO. Conditions: Initial SSY Concentration = 8 mg/L, ZnO Catalyst Loading = 7 g/L. Inset Shows the Decolourisation of SSY Dye Solution in 120 min under Optimised Operational Parameters.

From the result, the photocatalytic experiment at pH 5.8 exhibited the highest degradation efficiency and complete degradation was achieved after 120 min irradiation. On the other hand, slightly lower degradation efficiency was observed at pH 10.5 (94.9 %) and a much lower efficiency was observed at pH 3.1 (77 %) and pH 6.7 (75.5 %). The degradation efficiency was related to the properties of the dye molecules and catalyst. The pH of zero point charge (pH_{zpc}) for ZnO was reported to be 9.3. This meant that the photocatalyst surface was negatively charged when the pH was higher than pH_{zpc} and positively charged when the pH was lower than the pH_{zpc} (Lam et al, 2012; El-Sheikh & Al-Degs, 2013; Nollet & Toldra, 2015). On the other hand, the SSY is an anionic dye which is negatively charged (Horowitz et al, 2005; Fazeli, Sohrabi, & Tehrani-Bagha, 2012). Therefore, at pH 5.8, the electrostatic attraction between positively charged ZnO surface with anionic SSY resulted in high degradation efficiency of SSY.

At pH 3.1, the presence of sulphate anions (SO_4^{2-}) in the solution from H_2SO_4 can adsorb on the surface of the catalyst which led to lesser active sites and subsequestly lesser generation of active radicals (Liang et al, 2008; Sin et al, 2013). Thus, it led to lower degradation efficiency. Wei et al (2009) also found similar observation on the photocatalytic degradation of methyl orange over ITO/CdS/ZnO interface composite films. They reported that the degradation efficiency of dye decreased in the presence of SO_4^{2-} anions. It was due to the adsorbed SO_4^{2-} anions can scavenge the holes and •OH to produce less reactive sulphate radicals ($SO_4\bullet^-$) as shown in Equations (4.1) and (4.2) (Kashif & Ouyang, 2009; Wei et al, 2009).

$$SO_4^{2-} + h_{vb}^{+} \rightarrow SO_4\bullet^- \quad (4.1)$$

$$SO_4^{2-} + \bullet OH \rightarrow SO_4\bullet^- + OH^- \quad (4.2)$$

At pH 6.7, the presence of Na^+ ions from NaOH can compete with dye molecules for the active site on catalyst surface. Similar studies were also reported that ions from NaOH salts can compete with substrate molecules for adsorption on the catalyst surface of photocatalytic reaction thus this resulted in lower photocatalytic activity (Bekkouche et al. 2004; Sin et al, 2013; Preethi, Prithika & Yamini, 2015). At higher pH of 10.5, the photocatalytic efficiency of SSY was lower than pH 5.8 due to the electrostatic repulsion between both negatively charged ZnO and anionic SSY. However, the large amount of OH^- can react with holes to form

•OH radicals to attack the dye molecules. Thus, photocatalytic activity at pH 10.5 was higher than pH 3.1 and 6.7. Kansal & Kaur & Singh (2009) had similar observation when investigating the photocatalytic degradation of reactive orange 4 dye using ZnO photocatalyst. They stated that the high concentration of OH^- ions led to the generation of more •OH for organic pollutants degradation. Thus, high degradation efficiency was observed (Kansal & Kaur & Singh, 2009).

4.4 Scavenger Test

It was well-documented that active species including holes (h_{vb}^+), hydroxyl radicals (•OH) and super oxide anion radicals ($O_2•^-$) were involved in photocatalysis (Rauf & Ashraf, 2009; Ahmed et al, 2010; Lam et al, 2012; Ribeiro et al, 2015). In this study, ethanol was added as a scavenger of •OH radicals. Ethanol has been generally used as •OH radicals scavenger to estimate the oxidation mechanism due to its high rate constant of reaction between •OH radicals and ethanol (Daneshvar, Salari & Khataee, 2004; Xian et al, 2014). On the other hand, sodium oxalate was used to scavenge h_{vb}^+ due to its efficient formation of CO_2 and $CO_2•^-$ as in the reaction sequence shown below (Equation 4.3) (Jin et al, 2004; Wang et al, 2015). To investigate the effect of $O_2•^-$ radicals in the photcatalysis, 1,4-benzoquinone was introduced to the photocatalytic process due to its ability to trap these radicals by electron transfer mechanism (Equation 4.4) Misiaszek et al, 2004; Pelaez et al, 2012; Yang et al, 2013). Therefore, different scavengers were added on the degradation of SSY to remove the corresponding active species so the role of different active species in the photocatalytic process could be understood. The results of SSY photcatalytic degradation over ZnO photocatalyst in the presence of different scavengers at 2 mM are shown in Figure 4.8. All experiments were carried out with initial SSY concentration of 8 mg/L, catalyst loading of 7 g/L and solution pH of 5.8.

$$C_2O_4^{2-} + h_{vb}^+ \rightarrow CO_2 + CO_2•^- \quad (4.3)$$

$$O_2•^- + BQ \rightarrow O_2 + BQ• \quad (4.4)$$

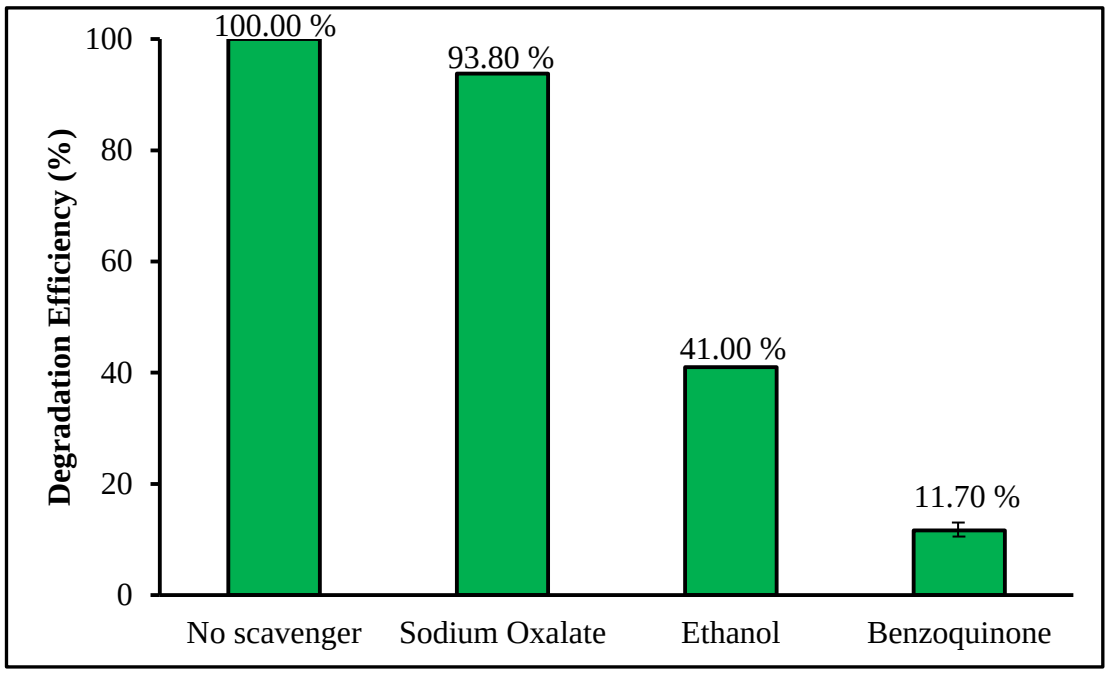

Figure 4.8: Effect of Different Scavengers at 2 mM on Photocatalytic Degradation of SSY dye over ZnO Photocatalysts. Conditions: Initial SSY concentration = 8 mg/L, ZnO Catalyst Loading = 7 g/L, solution pH = 5.8

As can be seen, the photocatalytic reaction of SSY degradation was suppressed as a consequence of radical scavenging. The degradation efficiencies of SSY decreased from 100 % to 41 %, 11.7 % and 93.8 % for ethanol, benzoquinone, and sodium oxalate, respectively after 120 min irradiation. It showed the participation of all radicals in the reaction mechanism. Among the radicals, $O_2\bullet^-$ radicals played more important role than the h_{vb}^+ and •OH radicals in the photocatalytic reaction in these present experiments. Similar result was also reported by Weng et al (2014) on the photocatalytic degradation of Rhodamine B using ZnO nano spheres. Their result showed that benzoquinone reduced the degradation efficiency significantly from 44 % to 4 % as compared to sodium oxalate (44 % to 9 %) and ethanol (44 % to 7 %) (Weng et al, 2014). In addition, Sun et al (2013) also had similar observation in the photocatalytic degradation of Rhodamine B using ZnO-based photocatalysts under irradiation of visible light. They reported that the presence of benzoquinone reduced the degradation efficiency from 62 % to 10 % as

compared to sodium oxalate (62 % to 56 %) and ethanol (62 % to 37 %) (Sun et al, 2013).

CHAPTER 5

CONCLUSION AND RECOMMENDATIONS

5.1 Conclusion

In this study, zinc oxide (ZnO) photocatalysts have been characterized and the photocatalytic degradation of sunset yellow (SSY) dye has been investigated. The fourier transform infrared (FTIR) spectrum of ZnO photocatalysts revealed the presence of Zn-O bonding which can prove the identity of the photocatalysts as ZnO semiconductor. The X-ray diffraction (XRD) pattern showed that the photocatalysts were hexagonal wurzite structured which was the typical structure of ZnO. In addition, no other crystalline impurities were observed in the pattern, thus the ZnO photocatalysts have high purity. The transmission electron microscopy (TEM) image of the ZnO nanoparticles revealed that the particles were irregularly shaped. The image also indicated the particle size range was from 153 nm to 283 nm

The control experiment of the SSY removal has shown high degradation efficiency was obtained under the combination of light and photocatalysts. Furthermore, it showed that the reactions in this study were indeed photocatalysis. The operating parameters that have been studied were initial SSY concentration, ZnO catalyst loading, and solution pH. The results showed that the degradation efficiency decreases as the initial SSY concentration increased. The optimal ZnO loading of 7 g/L was needed to obtain a high degradation efficiency of SSY. Unadjusted solution pH of SSY was favourable for photocatalytic degradation and optimum pH was found to be 5.8.

The scavenger test was carried out in order to determine the role of different active species in the photocatalytic degradation of SSY over ZnO nanoparticles under fluorescent light irradiation. The degradation efficiency was found to be decreased with the presence of any scavenger. This indicates that all three active species participated in the reaction. Among the active species, the superoxide anions ($O_2^{\bullet -}$) radicals played the major role as the SSY degradation was significantly suppressed in the presence of benzoquinone. The degradation efficiency decreased from 100 % to 11 % as compared to the 41 % and 93.8 % for the addition of ethanol and sodium oxalate, respectively.

5.2 Recommendations

A few recommendations were drawn for future research:

1) In this study, heterogeneous photocatalyst using commercial ZnO nanoparticles has been shown to provide an effective method to degrade organic dyes. For future work, synthesized ZnO nano photocatalysts to study their effect on photocatalysis should be considered.

2) Current study on the effects of operating parameters such as initial substrate concentration, catalyst loading and solution pH has been shown significantly affected the photocatalytic degradation. However, the effects of light intensity, inorganic anion and cation, the presence of oxidizing agents and air flow rate were not yet evaluated on this aspect. Thus, a systematic study should be carried out to study these effects.

3) Total organic carbon concentration of degraded dye pollutants should also be analysed to study the mineralization efficiency.

REFERENCES

Afroz, R., Masud, M., Akhtar, R. and Duasa, J. (2014). Water Pollution: Challenges and Future Direction for Water Resource Management Policies in Malaysia. *Environment and Urbanization Asia*, 5, 63-81.

Ahmed, S., Rasul, M., Martens, W., Brown, R. and Hashib, M. (2010). Heterogeneous photocatalytic degradation of phenols in wastewater: A review on current status and developments. *Desalination*, 261, 3-18.

Akyol, A. and Bayramoglu, M. (2005). Photocatalytic degradation of Remazol Red F3B using ZnO catalyst. *Journal of Hazardous Materials*, 124, 241-246.

Allegre, C., Maisseu, M., Charbit, F. and Moulin, P. (2004). Coagulation–flocculation–decantation of dye house effluents: concentrated effluents. *Journal of Hazardous Materials*, 116, 57-64.

All ègre, C., Moulin, P., Maisseu, M. and Charbit, F. (2006). Treatment and reuse of reactive dyeing effluents. *Journal of Membrane Science*, 269, 15-34.

Annadurai, G., Sivakumar, T. and Rajesh Babu, S. (2000). Photocatalytic decolorization of congo red over ZnO powder using Box-Behnken design of experiments. *Bioprocess Engineering*, 23, 0167-0173.

Azbar, N., Yonar, T. and Kestioglu, K. (2004). Comparison of various advanced oxidation processes and chemical treatment methods for COD and color removal from a polyester and acetate fiber dyeing effluent. *Chemosphere*, 55, 35-43.

Azizi, S., Ahmad, M., Namvar, F. and Mohamad, R. (2014). Green biosynthesis and characterization of zinc oxide nanoparticles using brown marine macroalga Sargassum muticum aqueous extract. *Materials Letters*, 116, 275-277.

Banerjee, P., DasGupta, S. and De, S. (2007). Removal of dye from aqueous solution using a combination of advanced oxidation process and nanofiltration. *Journal of Hazardous Materials*, 140, 95-103.

Bekkouche, S., Bouhelassa, M., Salah, N. and Meghlaoui, F. (2004). Study of adsorption of phenol on titanium oxide (TiO_2). *Desalination*, 166, 355-362.

Byrappa, K., Subramani, A., Ananda, S., Rai, K., Dinesh, R. and Yoshimura, M. (2006). Photocatalytic degradation of rhodamine B dye using hydrothermally synthesized ZnO. *Bulletin of Materials Science*, 29, 433-438.

Chakrabarti, S. and Dutta, B. (2004). Photocatalytic degradation of model textile dyes in wastewater using ZnO as semiconductor catalyst. *Journal of Hazardous Materials*, 112, 269-278.

Chen, C., Liu, J., Liu, P. and Yu, B. (2011). Investigation of Photocatalytic Degradation of Methyl Orange by Using Nano-Sized ZnO Catalysts. *ACES*, 01(01), 9-14.

Chen, T., Chang, I., Yang, M., Chiu, H. and Lee, C. (2013). The exceptional photo-catalytic activity of ZnO/RGO composite via metal and oxygen vacancies. *Applied Catalysis B: Environmental*, 142-143, 442-449.

Choo, H., Lam, S., Sin, J. and Mohamed, A. (2015). An efficient Ag_2SO_4 -deposited ZnO in photocatalytic removal of indigo carmine and phenol under outdoor light irradiation. *Desalination and Water Treatment*, 1-14.

Chong, M., Jin, B., Chow, C. and Saint, C. (2010). Recent developments in photocatalytic water treatment technology: A review. *Water Research*, 44, 2997-3027.

Comparelli, R., Fanizza, E., Curri, M., Cozzoli, P., Mascolo, G. and Agostiano, A. (2005). UV-induced photocatalytic degradation of azo dyes by organic-capped ZnO nanocrystals immobilized onto substrates. *Applied Catalysis B: Environmental*, 60, 1-11.

Daneshvar, N., Rasoulifard, M., Khataee, A. and Hosseinzadeh, F. (2007). Removal of C.I. Acid Orange 7 from aqueous solution by UV irradiation in the presence of ZnO nanopowder. *Journal of Hazardous Materials*, 143, 95-101.

Daneshvar, N., Salari, D. and Khataee, A. (2004). Photocatalytic degradation of azo dye acid red 14 in water on ZnO as an alternative catalyst to TiO_2. *Journal of Photochemistry and Photobiology A: Chemistry*, 162, 317-322.

Department of Environment, (2015). *River Water Pollution Sources | Department of Environment*. [online] Available at: http://www.doe.gov.my/portalv1/en/info-umum/punca-punca-kepada-pencemaran-air-sungai/278 [Accessed 25 Jun. 2015].

Dutta, S. and Ganguly, B. (2012). Characterization of ZnO nanoparticles grown in presence of Folic acid template. *Journal of Nanobiotechnology*, 10(1), 29.

El-Sheikh, A.H. and Al-Degs, Y.S. (2013). Spectrophotometric determination of food dyes in soft drinks by second order multivariate calibration of the absorbance spectra-pH data matrices. *Dyes and Pigments*, 97(2), 330-339.

Fazeli, S., Sohrabi, B. and Tehrani-Bagha, A. (2012). The study of Sunset Yellow anionic dye interaction with gemini and conventional cationic surfactants in aqueous solution. *Dyes and Pigments*, 95(3), 768-775.

Forgacs, E., Cserháti, T. and Oros, G. (2004). Removal of synthetic dyes from wastewaters: a review.*Environment International*, 30, 953-971.

Gao, B., Yue, Q., Wang, Y. and Zhou, W. (2007). Color removal from dye-containing wastewater by magnesium chloride. *Journal of Environmental Management*, 82, 167-172.

Gaya, U. and Abdullah, A. (2008). Heterogeneous photocatalytic degradation of organic contaminants over titanium dioxide: A review of fundamentals, progress and problems. *Journal of Photochemistry and Photobiology C: Photochemistry Reviews*, 9, 1-12.

Ghoneim, M., El-Desoky, H. and Zidan, N. (2011). Electro-Fenton oxidation of Sunset Yellow FCF azo-dye in aqueous solutions. *Desalination*, 274, 22-30.

Golob, V., Vinder, A. and Simonic, M. (2005). Efficiency of the coagulation/flocculation method for the treatment of dyebath effluents. *Dyes and Pigments*, 67, 93-97.

Gomes, K., Oliveira, M., Carvalho, F., Menezes, C. and Peron, A. (2013). Citotoxicity of food dyes sunset yellow (E-110), bordeaux red (E-123), and tatrazine yellow (E-102) on Allium cepa L. root meristematic cells. *Food Science and Technology (Campinas)*, 33, 218-223.

Gusatti, M., Barroso, G., Campos, C., Souza, D., Rosário, J., Lima, R., Milioli, C., Silva, L., Riella, H. and Kuhnen, N. (2011). Effect of different precursors in the chemical synthesis of ZnO nanocrystals. *Mat. Res.*, 14(2), 264-267.

Hariharan, C. (2006). Photocatalytic degradation of organic contaminants in water by ZnO nanoparticles: Revisited. *Applied Catalysis A: General*, 304, 55-61.

Hayat, K., Gondal, M., Khaled, M. and Ahmed, S. (2010). Kinetic study of laser-induced photocatalytic degradation of dye (alizarin yellow) from wastewater using nanostructured ZnO. *Journal of Environmental Science and Health, Part A*, 45, 1413-1420.

Horowitz, V., Janowitz, L., Modic, A., Heiney, P. and Collings, P. (2005). Aggregation behavior and chromonic liquid crystal properties of an anionic monoazo dye. *Physical Review E*, 72(4).

Hong, R., Pan, T., Qian, J. and Li, H. (2006). Synthesis and surface modification of ZnO nanoparticles.*Chemical Engineering Journal*, 119, 71-81.

Hong, R., Qian, J. and Cao, J. (2006). Synthesis and characterization of PMMA grafted ZnO nanoparticles. *Powder Technology*, 163(3), 160-168.

Hunger, K. (2003). *Industrial dyes*. Weinheim, Wiley-VCH.

Jiang, Y., Sun, Y., Liu, H., Zhu, F. and Yin, H. (2008). Solar photocatalytic decolorization of C.I. Basic Blue 41 in an aqueous suspension of TiO_2–ZnO. *Dyes and Pigments*, 78(1), pp.77-83.

Jin, R., Gao, W., Chen, J., Zeng, H., Zhang, F., Liu, Z. and Guan, N. (2004). Photocatalytic reduction of nitrate ion in drinking water by using metal-loaded $MgTiO_3$-TiO_2 composite semiconductor catalyst. *Journal of Photochemistry and Photobiology A: Chemistry*, 162(2-3), 585-590.

Jo, W. and Tayade, R. (2014). Recent developments in photocatalytic dye degradation upon irradiation with energy-efficient light emitting diodes. *Chinese Journal of Catalysis*, 35, 1781-1792.

Joo, J., Ahn, C., Jang, D., Yoon, Y., Kim, J., Campos, L. and Ahn, H. (2013). Photocatalytic degradation of trichloroethylene in aqueous phase using nano-ZnO/Laponite composites. *Journal of Hazardous Materials*, 263, 569-574.

Kansal, S., Hassan Ali, A. and Kapoor, S. (2010). Photocatalytic decolorization of biebrich scarlet dye in aqueous phase using different nanophotocatalysts. *Desalination*, 259, 147-155.

Kansal, S., Kaur, N. and Singh, S. (2009). Photocatalytic Degradation of Two Commercial Reactive Dyes in Aqueous Phase Using Nanophotocatalysts. *Nanoscale Res Lett*, 4, 709-716.

Kashif, N. and Ouyang, F. (2009). Parameters effect on heterogeneous

photocatalysed degradation of phenol in aqueous dispersion of TiO_2. *Journal of Environmental Sciences*, 21(4), 527-533.

Kazeminezhad, I. and Sadollahkhani, A. (2014). Photocatalytic degradation of Eriochrome black-T dye using ZnO nanoparticles. *Materials Letters*, 120, 267-270.

Khouni, I., Marrot, B., Moulin, P. and Ben Amar, R. (2011). Decolourization of the reconstituted textile effluent by different process treatments: Enzymatic catalysis, coagulation/flocculation and nanofiltration processes. *Desalination*, 268, 27-37.

Krishnakumar, B., Imae, T., Miras, J. and Esquena, J. (2014). Synthesis and azo dye photodegradation activity of ZrS_2-ZnO nano-composites. *Separation and Purification Technology*, 132, 281-288.

Kumar, S., Venkateswarlu, P., Rao, V. and Rao, G. (2013). Synthesis, characterization and optical properties of zinc oxide nanoparticles. *Int Nano Lett*, 3, 30.

Lam, S., Sin, J., Abdullah, A. and Mohamed, A. (2012). Degradation of wastewaters containing organic dyes photocatalysed by zinc oxide: a review. *Desalination and Water Treatment*, 41, 131-169.

Lai, Y., Meng, M., Yu, Y., Wang, X. and Ding, T. (2011). Photoluminescence and photocatalysis of the flower-like nano-ZnO photocatalysts prepared by a facile hydrothermal method with or without ultrasonic assistance. *Applied Catalysis B: Environmental*, 105(3-4), 335-345.

Lenntech.com, (2015). *Water pollutant information FAQ*. [online] Available from: http://www.lenntech.com/water-pollutants-faq.htm# [Accessed 27 Jun. 2015].

Liang, H., Li, X., Yang, Y. and Sze, K. (2008). Effects of dissolved oxygen, pH, and anions on the 2,3-dichlorophenol degradation by photocatalytic reaction with anodic TiO2 nanotube films. *Chemosphere*, 73(5), 805-812.

Long, T., Yin, S., Takabatake, K., Zhnag, P. and Sato, T. (2008). Synthesis and Characterization of ZnO Nanorods and Nanodisks from Zinc Chloride Aqueous Solution. *Nanoscale Res Lett*, 4(3), 247-253.

Matei, A., Cernica, I., Cadar, O., Roman, C. and Schiopu, V. (2008). Synthesis and characterization of ZnO – polymer nanocomposites. *International Journal of Material Forming*, 1(S1), 767-770.

Mekasuwandumrong, O., Pawinrat, P., Praserthdam, P. and Panpranot, J. (2010). Effects of synthesis conditions and annealing post-treatment on the photocatalytic activities of ZnO nanoparticles in the degradation of methylene blue dye. *Chemical Engineering Journal*, 164, 77-84.

Misiaszek, R., Crean, C., Joffe, A., Geacintov, N. and Shafirovich, V. (2004). Oxidative DNA Damage Associated with Combination of Guanine and Superoxide Radicals and Repair Mechanisms via Radical Trapping. *Journal of Biological Chemistry*, 279(31), 32106-32115.

Mittal, A. (2011). Biological Wastewater Treatment. *Water Today* [Online] Available from: http://www.watertoday.org/Article%20Archieve/Aquatech%2012.pdf [Accessed 26 Jun. 2015].

Moafi, H., Zanjanchi, M. and Shojaie, A. (2013). Tungsten-doped ZnO nanocomposite: Synthesis, characterization, and highly active photocatalyst toward dye photodegradation. *Materials Chemistry and Physics*, 139, 856-864.

Modirshahla, N., Hassani, A., Behnajady, M. and Rahbarfam, R. (2011). Effect of operational parameters on decolorization of Acid Yellow 23 from wastewater by UV irradiation using ZnO and ZnO/SnO_2 photocatalysts. *Desalination*, 271, 187-192.

Mohaghegh, N., Tasviri, M., Rahimi, E. and Gholami, M. (2014). Nano sized ZnO composites: Preparation, characterization and application as photocatalysts for degradation of AB92 azo dye. *Materials Science in Semiconductor Processing*, 21, 167-179.

Mohsin, D., Juda, A. and Mashkour, M. (2013). Thermodynamic and Kinetic Study for Aromatic Rings Effect on The Photooxidation rate. *International Journal of Engineering & Technology IJET-IJENS*, 13(4), 34-40.

Mrowetz, M. and Selli, E. (2006). Photocatalytic degradation of formic and benzoic acids and hydrogen peroxide evolution in TiO_2 and ZnO water suspensions. *Journal of Photochemistry and Photobiology A: Chemistry*, 180, 15-22.

Nishio, J., Tokumura, M., Znad, H. and Kawase, Y. (2006). Photocatalytic decolorization of azo-dye with zinc oxide powder in an external UV light irradiation slurry photoreactor. *Journal of Hazardous Materials*, 138, 106-115.

Nollet, L. and Toldra, F. (2015). *Handbook of Food Analysis, Third Edition - Two Volume Set*. 3rd ed. CRC Press, 121.

Pal, B., Sarkar, D. and Giri, P. (2015). Structural, optical, and magnetic properties of Ni doped ZnO nanoparticles: Correlation of magnetic moment with defect density. *Applied Surface Science*, 356, 804-811.

Pandey, A., Singh, P. and Iyengar, L. (2007). Bacterial decolorization and degradation of azo dyes.*International Biodeterioration & Biodegradation*, 59, 73-84.

Pelaez, M., Nolan, N., Pillai, S., Seery, M., Falaras, P., Kontos, A., Dunlop, P., Hamilton, J., Byrne, J., O'Shea, K., Entezari, M. and Dionysiou, D. (2012). A review on the visible light active titanium dioxide photocatalysts for environmental applications. *Applied Catalysis B: Environmental*, 125, 331-349.

Preethi, M., Prithika, S. and Yamini, R. (2015). Solar Light Aided Photobleaching of Congo red Dye Using Spions: a Novel Route for Complete Dye Degradation. *International Journal of Innovative Research in Science, Engineering and Technology*, 4(1), 101-111.

Punzi, M., Mattiasson, B. and Jonstrup, M. (2012). Treatment of synthetic textile wastewater by homogeneous and heterogeneous photo-Fenton oxidation. *Journal of Photochemistry and Photobiology A: Chemistry*, 248, 30-35.

Rahman, Q., Ahmad, M., Misra, S. and Lohani, M. (2013). Effective photocatalytic degradation of rhodamine B dye by ZnO nanoparticles. *Materials Letters*, 91, 170-174.

Rajamanickam, D., Dhatshanamurthi, P. and Shanthi, M. (2015). Preparation and characterization of SeO_2/TiO_2 composite photocatalyst with excellent performance for sunset yellow azo dye degradation under natural sunlight illumination. *Spectrochimica Acta Part A: Molecular and Biomolecular Spectroscopy*, 138, 489-498.

Rao, A., Sivasankar, B. and Sadasivam, V. (2009). Kinetic studies on the photocatalytic degradation of Direct Yellow 12 in the presence of ZnO catalyst. *Journal of Molecular Catalysis A: Chemical*, 306, 77-81.

Rao, D.G., Senthilkumar, R., Anthony Byrne, J., Feroz, S. (2012). *Wastewater Treatment: Advanced Processes and Technologies*. IWA Publishing, 49.

Raoufi, D. (2013). Synthesis and microstructural properties of ZnO nanoparticles prepared by precipitation method. *Renewable Energy*, 50, 932-937.

Rauf, M. and Ashraf, S. (2009). Fundamental principles and application of heterogeneous photocatalytic degradation of dyes in solution. *Chemical Engineering Journal*, 151, 10-18.

Ribeiro, A., Nunes, O., Pereira, M. and Silva, A. (2015). An overview on the advanced oxidation processes applied for the treatment of water pollutants defined in the recently launched Directive 2013/39/EU. *Environment International*, 75, 33-51.

Riera-Torres, M., Gutiérrez-Bouzán, C. and Crespi, M. (2010). Combination of coagulation–flocculation and nanofiltration techniques for dye removal and water reuse in textile effluents.*Desalination*, 252, 53-59.

Sabnis, R. (2010). *Handbook of biological dyes and stains*. John Wiley & Sons, 450.

Sakthivel, S., Neppolian, B., Shankar, M., Arabindoo, B., Palanichamy, M. and Murugesan, V. (2002). Solar photocatalytic degradation of azo dye: comparison of photocatalytic efficiency of ZnO and TiO_2. *Solar Energy Materials and Solar Cells*, 77, 65-82.

Sanna, V., Pala, N., Alzari, V., Nuvoli, D. and Carcelli, M. (2015). ZnO nanoparticles with High degradation efficiency of organic dyes under sunlight irradiation. *Materials Letters*, 162, 257-260.

Santos, A. dos., Cervantes, F. and van Lier, J. (2007). Review paper on current technologies for decolourisation of textile wastewaters: Perspectives for anaerobic biotechnology. *Bioresource Technology*, 98, 2369-2385.

Saratale, R., Saratale, G., Chang, J. and Govindwar, S. (2011). Bacterial decolorization and degradation of azo dyes: A review. *Journal of the Taiwan Institute of Chemical Engineers*, 42, 138-157.

Seyed-Dorraji, M., Daneshvar, N. and Aber, S. (2009). Influence Of Inorganic Oxidants And Metal Ions On Photocatalytic Activity Of Prepared Zinc Oxide Nanocrystals. *Global NEST Journal*, 11(4), 535-545.

Sin, J., Lam, S., Lee, K. and Mohamed, A. (2013). Photocatalytic performance of novel samarium-doped spherical-like ZnO hierarchical nanostructures under visible light irradiation for 2,4-dichlorophenol degradation. *Journal of Colloid and Interface Science*, 401, 40-49.

Singh, R., Singh, P. and Singh, R. (2015). Enzymatic decolorization and degradation of azo dyes – A review. *International Biodeterioration & Biodegradation*, 104, 21-31.

Sun, W., Li, J., Mele, G., Zhang, Z. and Zhang, F. (2013). Enhanced photocatalytic degradation of rhodamine B by surface modification of ZnO with copper (II) porphyrin under both UV–vis and visible light irradiation. *Journal of Molecular Catalysis A: Chemical*, 366, 84-91.

Suresh, P., Vijaya, J. and Kennedy, L. (2014). Photocatalytic degradation of textile-dyeing wastewater by using a microwave combustion-synthesized zirconium oxide supported activated carbon.*Materials Science in Semiconductor Processing*, 27, 482-493.

The Commissioner of Law Revision, Malaysia, (2006). *Environmental Quality Act 1974*. [Online] Official Portal of Attorney General's Chambers of Malaysia. Available from: http://www.agc.gov.my/Akta/Vol.%203/Act%20127.pdf [Accessed 27 Jun. 2015].

Umar, A., Kumar, R., Kumar, G., Algarni, H. and Kim, S. (2015). Effect of annealing temperature on the properties and photocatalytic efficiencies of ZnO nanoparticles. *Journal of Alloys and Compounds*, 648, 46-52.

United States Environmental Protection Agency, (1999). Wastewater Technology Fact Sheet Ozone Disinfection. *EPA*. [Online] Available from: http://water.epa.gov/scitech/wastetech/upload/2002_06_28_mtb_ozon.pdf [Accessed 27 Jun. 2015].

Velmurugan, R. and Swaminathan, M. (2011). An efficient nanostructured ZnO for dye sensitized degradation of Reactive Red 120 dye under solar light. *Solar Energy Materials and Solar Cells*, 95, 942-950.

Verma, A., Dash, R. and Bhunia, P. (2012). A review on chemical coagulation/flocculation technologies for removal of colour from textile wastewaters. *Journal of Environmental Management*, 93, 154-168.

Vijayaprasath, G., Murugan, R., Palanisamy, S., Prabhu, N., Mahalingam, T., Hayakawa, Y. and Ravi, G. (2016). Role of nickel doping on structural, optical, magnetic properties and antibacterial activity of ZnO nanoparticles. *Materials Research Bulletin*, 76, 48-61.

Wahab, R., Ansari, S., Kim, Y., Seo, H., Kim, G., Khang, G. and Shin, H. (2007). Low temperature solution synthesis and characterization of ZnO nano-flowers. *Materials Research Bulletin*, 42(9), 1640-1648.

Wang, W., Huang, G., Yu, J. and Wong, P. (2015). Advances in photocatalytic disinfection of bacteria: Development of photocatalysts and mechanisms. *Journal of Environmental Sciences*, 34, 232-247.

Wei, S., Shao, Z., Lu, X., Liu, Y., Cao, L. and He, Y. (2009). Photocatalytic degradation of methyl orange over ITO/CdS/ZnO interface composite films. *Journal of Environmental Sciences*, 21(7), 991-996.

Weng, B., Yang, M., Zhang, N. and Xu, Y. (2014). Toward the enhanced photoactivity and photostability of ZnO nanospheres via intimate surface coating with reduced graphene oxide. *J. Mater. Chem. A*, 2(24), 9380.

Wwf.panda.org, (2015). *Water Pollution*. [online] Available from: http://wwf.panda.org/about_our_earth/teacher_resources/webfieldtrips/water_pollution/ [Accessed 26 Jun. 2015].

Xian, T., Yang, H., Di, L., Ma, J., Zhang, H. and Dai, J. (2014). Photocatalytic reduction synthesis of $SrTiO_3$-graphene nanocomposites and their enhanced photocatalytic activity. *Nanoscale Res Lett*, 9(1), 327.

Xie, J., Li, Y., Zhao, W., Bian, L. and Wei, Y. (2011). Simple fabrication and photocatalytic activity of ZnO particles with different morphologies. *Powder Technology*, 207, 140-144.

Xie, W., Li, Y., Sun, W., Huang, J., Xie, H. and Zhao, X. (2010). Surface modification of ZnO with Ag improves its photocatalytic efficiency and photostability. *Journal of Photochemistry and Photobiology A: Chemistry*, 216, 149-155.

Xiong, G., Pal, U., Serrano, J., Ucer, K. and Williams, R. (2006). Photoluminesence and FTIR study of ZnO nanoparticles: the impurity and defect perspective. *phys. stat. sol. (c)*, 3(10), 3577-3581.

Xu, W., Liu, S., Lu, S., Kang, S., Zhou, Y. and Zhang, H. (2010). Photocatalytic degradation in aqueous solution using quantum-sized ZnO particles supported on sepiolite. *Journal of Colloid and Interface Science*, 351, 210-216.

Yang, J., Liu, X., Yang, L., Wang, Y., Zhang, Y., Lang, J., Gao, M. and Wei, M. (2009). Effect of different annealing atmospheres on the structure and optical properties of ZnO nanoparticles. *Journal of Alloys and Compounds*, 485(1-2), 743-746.

Yang, L., Dong, S., Sun, J., Feng, J., Wu, Q. and Sun, S. (2010). Microwave-assisted preparation, characterization and photocatalytic properties of a dumbbell-shaped ZnO photocatalyst. *Journal of Hazardous Materials*, 179(1-3), 438-443.

Yang, M., Zhang, Y., Zhang, N., Tang, Z. and Xu, Y. (2013). Visible-Light-Driven Oxidation of Primary C–H Bonds over CdS with Dual Co-catalysts Graphene and TiO_2. *Sci. Rep.*, 3, 3314.

Zangeneh, H., Zinatizadeh, A., Habibi, M., Akia, M. and Hasnain Isa, M. (2015). Photocatalytic oxidation of organic dyes and pollutants in wastewater using different modified titanium dioxides: A comparative review. *Journal of Industrial and Engineering Chemistry*, 26, 1-36.

Zhai, J., Tao, X., Pu, Y., Zeng, X. and Chen, J. (2010). Core/shell structured ZnO/SiO_2 nanoparticles: Preparation, characterization and photocatalytic property. *Applied Surface Science*, 257, 393-397.

APPENDIX

Appendix A

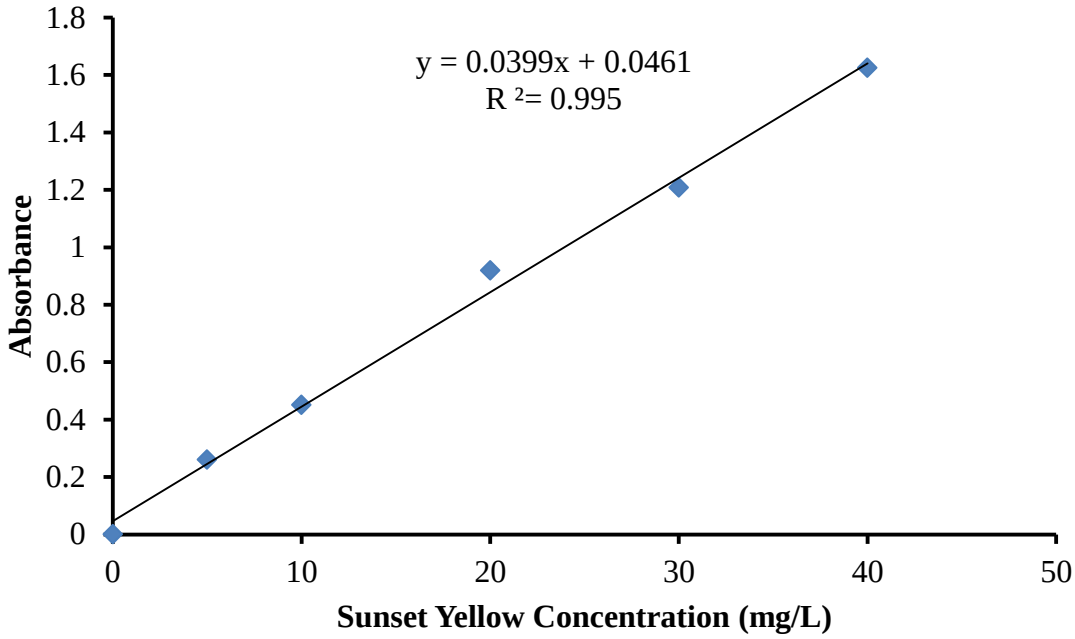

Appendix A: Uv-vis Spectrophotometer Calibration Line for Sunset Yellow (SSY) Concentration Versus Peak Area.